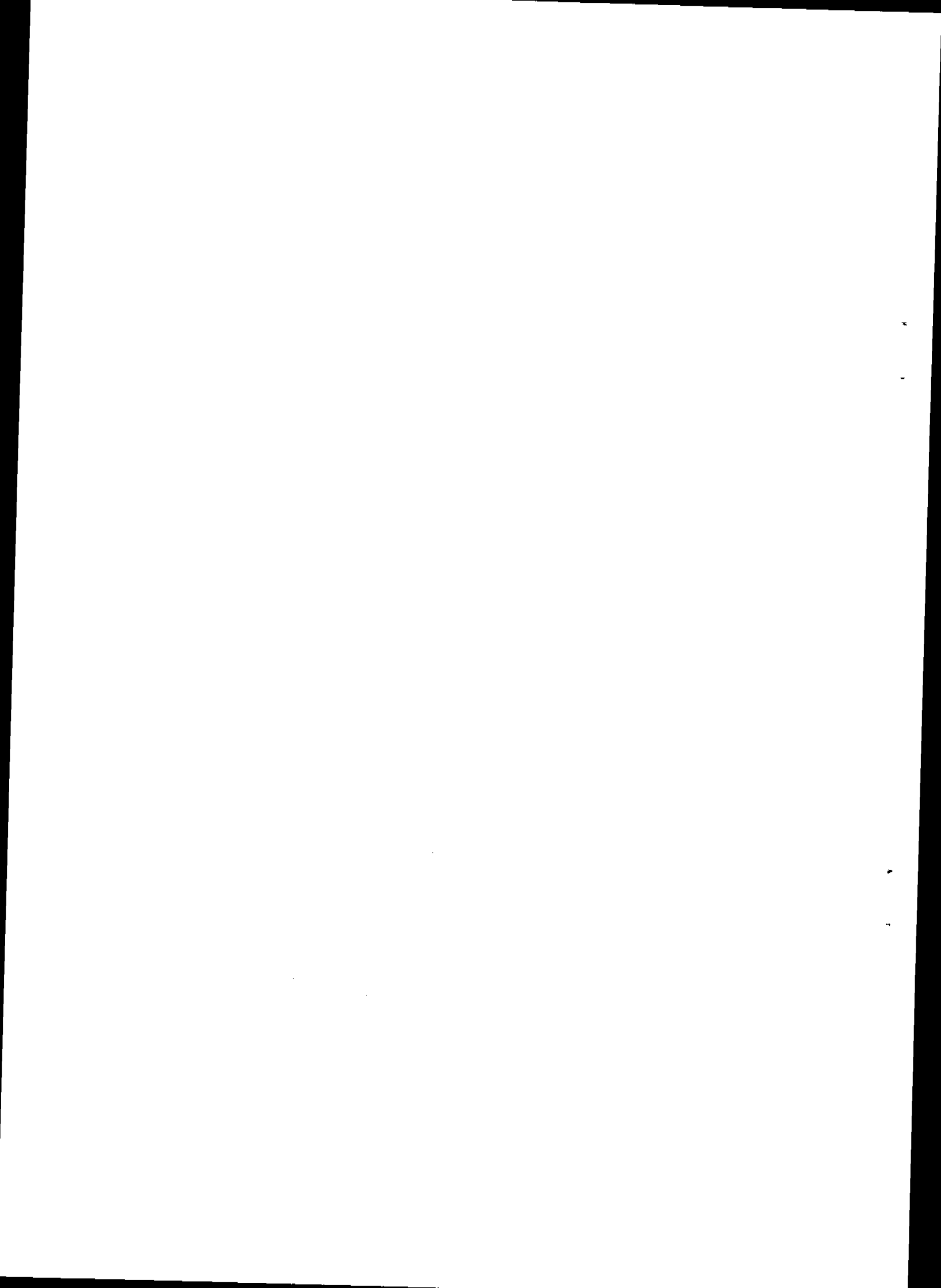


Jlab Experiment E93050
Virtual Compton Scattering

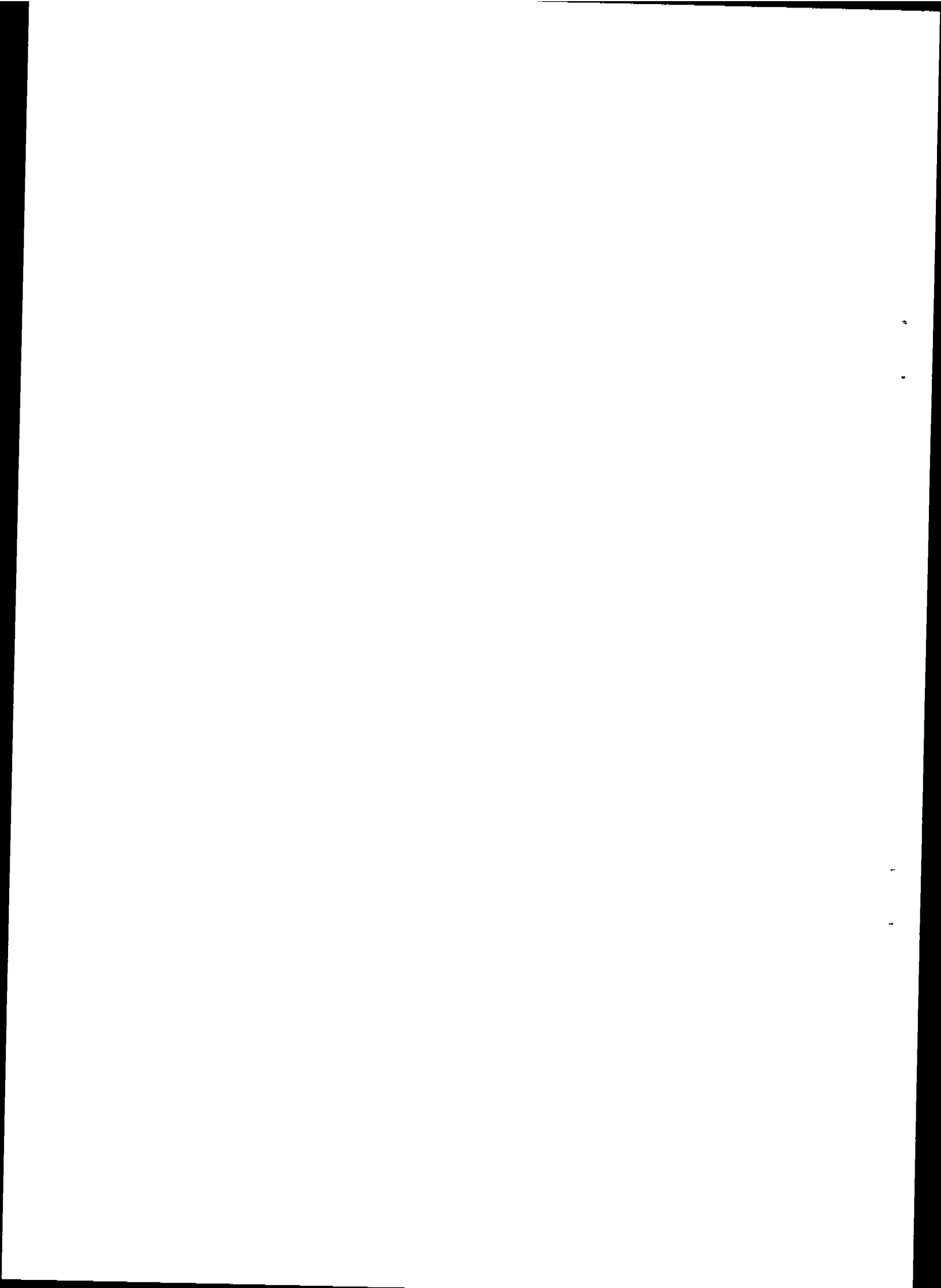
Technical Notes on Experimental Studies
1st Pass Analysis 1998-2000

S.Jaminion, H.Fonvieille
LPC-Clermont-Fd

For the Hall A VCS-Collaboration



Part I :	Hall A 15 cm Hydrogen Cryotarget: Absolute Positioning along Beam Axis	2 p.
Part II :	Proposition of procedure to make the choice of "calset" in the Electron arm Run per Run based on single-arm events (T1)	12 p.
Part III :	HRS Optics Optimization with extended targets	7 p.
Part IV :	a study of Optic Databases Resolution	18 p.



E93050

Hall A 15cm Hydrogen Cryotarget: Absolute Positioning along Beam Axis

*S. Jaminion, H. Fonvieille
LPC-Clermont-Fd, September 2000*

This note is an addendum to a previous report [1] which provided target positioning information, for empty targets used in calibration data of experiment E93050. One missing item was the same information, but for the 15cm long liquid hydrogen target used in physics data. The present report summarizes our knowledge on the subject.

1 Need for knowledge of target positioning

We have been using this information in 1st pass analysis in order to make spectrometer mispointing diagnostic: a comparison is made between the expected position of target endcaps along the beamline, and the ones obtained from event reconstruction.

Target length seen by the spectrometers: in E93050, the Electron arm always sees the whole target length, due to small spectrometer angle: 15° to 23° . The Hadron arm may or may not see the whole target, depending on the spectrometer angle, which goes from 54° to 38° (polarizabilities) or 18° (resonances). The transition region (length fully seen / not fully seen) is around 43° , as can be seen clearly from 15 cm empty target runs CA2-5.

Variables characterizing target position: the 15 cm long hydrogen cryotarget in Hall A is surveyed regularly, together with the other target cells, in order to check its position along the beamline. This position is given in the lab frame along the Z_{Hall} axis. It is characterized either by the Z-coordinate of target middle: Z_{middle} , or by the coordinate of the two endcaps: $Z_{upstream}$ and $Z_{downstream}$. The latter information is more practical for experimental analysis.

2 Data for 15 cm LH2 target

We used the survey measurements of March 13, 1998 [2]. The 15 cm LH2 target is called CRYO2T.

Warm survey:

$$\begin{aligned} (z \text{ values}) \quad & \text{CRYO2TA} = -0.07 \text{ mm} \\ & \text{CRYO2TB} = -0.37 \text{ mm} \\ & \text{CRYO2TC} = -0.38 \text{ mm} \\ & \text{CRYO2TD} = -0.24 \text{ mm} \end{aligned}$$

$$\Rightarrow \bar{z}_{\text{warm}} = -0.265 \text{ mm.}$$

\bar{z}_{warm} is the amount by which the target would have to be moved in order to be centered w.r.t. Hall A origin. It is equivalent to say that the position of the target middle is $Z_{\text{middle warm}} = +0.265$ mm in Hall A frame.

Cold survey:

When the targets got cold, the whole system moved upstream by 1.5 mm [3]. Then one gets: $Z_{\text{middle cold}} = -1.235$ mm. The (cold) target length is 149.5 mm [4] \Rightarrow

$$Z_{\text{upstream}} = -(149.5/2.) - 1.235 = -75.985 \text{ mm}$$

$$Z_{\text{downstream}} = +(149.5/2.) - 1.235 = +73.515 \text{ mm}$$

The overall uncertainty on these values is dominated by warm \rightarrow cold global motion uncertainty. It is likely to be of the order of ± 1 mm, or more conservatively ± 2 mm.

References

- [1] S.Jaminion, H.Fonvieille, " Y_{tg} optimization for E93050 Experiment", Report PCCF-RI-9816 (1998).
- [2] Target survey of Febr.13,1998 (emitted on March 13,1998).
- [3] J.P.Chen (Hall A) private communication (1998).
- [4] R.Suleiman, "Hall A Cryogenic and Dummy Targets Information", Jlab TN 97-008 (1997).

VCS-E93050

**Proposition of Procedure
to make the choice of "CALSET"
in the Electron Arm Run per Run
based on single Arm events (T1)**

H.Fonvieille, S.Jaminion

November 1999

1 Introduction

Reminder: the basic problem is that the **mispointing of the E-arm spectrometer**, in horizontal plane, w.r.t. origin of Hall A, is not determined unambiguously run per run.

This mispointing, measured along the y_{tg} axis of the spectrometer, is called “**HPMMAG**” in Javier Gomez’s code **survey**. It is normally determined from EPICS data, namely from the reading of a horizontal LVDT. In the electron arm, this measurement leads to two different values of mispointing because one can apply two different **calibration sets** to convert the measurement into HPMMAG in millimeters.

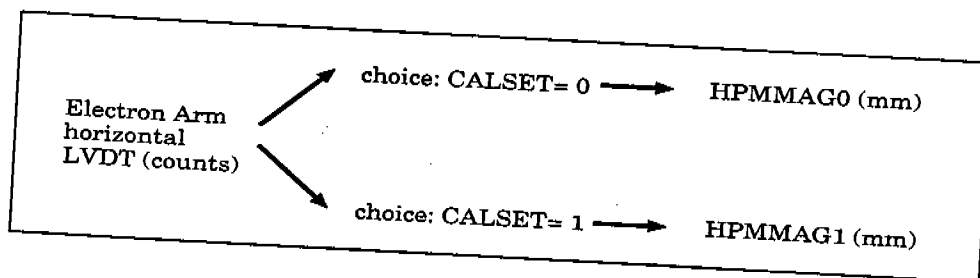


Figure 1:

To our present knowledge, HPMMAG0 and HPMMAG1 can differ by 1 to 3.5 millimeters. This is large compared to our goal of 0.5 mm accuracy in positioning, so it is important to use the true mispointing. The calibration set to apply for a given run is not known a priori. One has to determine it: this is what we call “**to make the choice of calset**” for this run.

Reliability of EPICS data: We believe that for most of the E93050 runs, one value among HPMMAG0 and HPMMAG1 is the true one. So the problem is just to select the right value among two possibilities. For a small number of runs, it may happen that none of the values HPMMAG0 or HPMMAG1 is reliable. In this case we have to find a method to determine the true mispointing, based on event analysis and physical observations.

This memo proposes a general method for solving the problem.

Below are listed some of the consequences of doing event analysis with a wrong E-arm spectrometer mispointing:

- the z-coordinate of the vertex point in the target is systematically biased: this is the case for the variables `twoarmz` and `spec.e.reactz` .
- the peak in `twoarmx-beamx` for true coincidences is not centered on zero.
- the peak in `(spec.e.reactz - spec.h.reactz)` for true coincidences is not centered on zero.

- if a wrong HPMMAG is introduced in the simulation of the experiment, the solid angle computed from the simulation has a systematic bias (and hence the cross section determination too). This is probably the most important consequence.

2 Why a single-arm method

To make the choice of calset for a given run, it is preferable to minimize the number of inputs which are not well known. This is why we propose a method based on **Electron Arm T1 events**, because it depends only on Electron optics database (Y and P elements) which is well established.

Throughout this memo, names of variables will always be implicitly attached to the Electron arm.

Other methods can be based on double-arm observables: such as the centering of (twoarmx-beamx) spectrum or (spec.e.reactz-spec.h.reactz) spectrum. But these methods depend also on Hadron optics database, which may introduce supplementary uncertainty.

The main condition to use the single-arm method is that the whole target length of 15cm is seen by the Electron spectrometer. This is indeed the case for spectrometer angles of 15.4° and 23.0°, i.e. for the polarizability data at $Q^2 = 1$ and 2 GeV².¹ One also needs reliable beam coordinates on target event by event: beamx and beamy. But this is true for other methods.

Another advantage is that the single-arm method is very simple in its principle and simple to use. It requires only a sample of clean T1 events with high enough statistics (≤ 200000 events).

3 Sensitivity of variables to spectrometer mispointing

For single-arm study of horizontal mispointing, one basically has the choice between two variables:

`y_tg` and `spec.e.reactz`

Both have advantages and disadvantages.

¹It is definitely NOT the case for spectrometer angles greater than 45°. Between 23 and 45 degrees it remains to be tested.

3.1 Working with y_{tg} :

- **Advantages:** y_{tg} is the most simple and direct variable one can think of. It is sensitive to the actual spectrometer mispointing, but it is insensitive to the choice of calset. From the experimental y_{tg} distribution, one can extract directly the actual value of HPMMAG and compare it to the two possibilities given by *survey+calset0* (HPMMAG0) and *survey+calset1* (HPMMAG1).
- **Disadvantages:** this determination of the actual HPMMAG from an experimental y_{tg} distribution is not completely straightforward and may not yield enough accuracy to disentangle between the two possibilities in some cases.

If during the experiment the spectrometer mispointing would truly change suddenly by 20 mm, the y_{tg} experimental distribution would be shifted suddenly by 20 mm. So in that sense the y_{tg} distribution is sensitive to the actual spectrometer mispointing.

But for a given run, conditions are generally stable. The spectrometer mispointing is what it is, it does not change, and the y_{tg} distribution obtained is unique. It does not depend on the choice of calset, which just reflects that we don't know if the actual mispointing was equal to HPMMAG0 or HPMMAG1. So in that sense the y_{tg} distribution is insensitive to the choice of calset. This is because y_{tg} is a quantity built intrinsically in the spectrometer frame. The spectrometer mispointing is a quantity which positions the spectrometer w.r.t. the outside world, e.g. the Hall A frame.

N.B: y_{tg} is very slightly sensitive to the choice of calset, due to the extended target corrections; see an example in figure 2. Indeed, to do these corrections one has to go from spectrometer frame to Hall A frame in order to compute a 3D vertex point.

The basic intuitive idea to determine the actual mispointing of the E-arm from an experimental y_{tg} distribution is that the "central value", or "middle" of this spectrum reflects the true value of HPMMAG. This simple vision is correct when *i*) the beam is well-centered w.r.t. Hall A origin (average beamx=0) ; *ii*) the target is well-centered w.r.t. Hall A origin (endcaps at + and - 75 mm); *iii*) the y_{tg} distribution is left-right symmetric, so that defining a middle is meaningful.

If the beam and/or target centering is not perfect but is known, one can take it into account. But we have encountered difficulties to define what is the middle of a distribution which may have asymmetric edges, or edges not straight enough to make a linear fit, and so on. Another problem is that the horizontal raster size contributes to the width of the experimental y_{tg} distribution. So it is not easy to verify that the whole target length is seen by the spectrometer just by looking at the y_{tg} spectrum.

So all in all the y_{tg} allows to disentangle between two possibilities HPMMAG0 and HPMMAG1 but only when these two values are different enough.

3.2 Working with spec_e.reactz:

- **Advantages:** *spec_e.reactz* is the true Z-coordinate of a vertex point. As such, it is easier to interpret in terms of physics and constraints, than y_{tg} . *spec_e.reactz* is insensitive to the actual mispointing of the spectrometer. But it is sensitive to the choice of calset. In fact it is the variable which has maximal sensitivity to the choice of calset.
- **Disadvantages:** *spec_e.reactz* is a variable much more elaborate than y_{tg} . It needs more knowledge of more quantities in order to be used reliably.

There is one simple and unambiguous constraint on the experimental distribution of *spec_e.reactz*: the Z-vertex must lie inside a 15cm window that is uniquely positioned in Hall A frame. In that sense *spec_e.reactz* is insensitive to the actual mispointing of the spectrometer.

As it represents a coordinate along the beam axis, it is insensitive to the width of the horizontal raster (contrary to y_{tg}). The *spec_e.reactz* spectrum reflects a target length along Z, and it allows to check that the whole target is seen by the spectrometer; see figures 3, 4 or 5.

spec_e.reactz is an analytic function of five variables: y_{tg} , ϕ_{tg} , *beamx*, HPMMAG and spectrometer angle. To build this variable reliably, one must have confidence in the Electron Arm optics (Y and P elements) and beam position event by event. Being an explicit function of HPMMAG, *spec_e.reactz* is sensitive to the choice of calset.

The sensitivity to the choice of calset is maximized for all variables computed along the beam axis. This is because, when going from the y_{tg} -axis to the Z-axis one has to multiply by a factor $1/\sin(\theta_{HRS})$. For the Electron arm at 15° , this makes an enhancement factor of 3.7^2 .

The basic idea is that, for the true value of spectrometer mispointing HPMMAG, the experimental *spec_e.reactz* spectrum should be well-centered w.r.t. the target survey. So by trying the two possibilities HPMMAG0 and HPMMAG1 one gets two distributions of *spec_e.reactz*, one well-centered and the other mis-centered.

The survey of the 15cm LH2 cryotarget gives endcaps positions in Hall A frame with finite accuracy. The main uncertainty comes from an observed shift along beam axis when cooling the target. We assumed an uncertainty of ± 1 mm due to this effect. This error bar is shown in figure 5.

²In double-arm methods there is the same kind of enhancement factor for (*spec_e.reactz-spec_h.reactz*) w.r.t. (*twoarm_x-beamx*).

3.3 To summarize:

study based on y_{tg}	study based on $spec.e.reactz$
one experimental spectrum of y_{tg} <i>to be compared to</i> two predictions of Y_{middle} (one for each calset)	two experimental spectra of $spec.e.reactz$ (one for each calset) <i>to be compared to</i> one prediction (from target survey)

4 Do we have confidence in the E-arm optics for this test of calset?

One may say: "you use E-arm optics to determine a choice of calset. But the E-arm optics itself has been optimized using a choice of calset. So you're inside a round loop and you find self-comforting results just like a snake biting its own tail."

To show that this is not the case, let's recall how historically we built the E-arm optics for E93050 in relation with the problem of calset choice.

a). we analyzed calibration data (ca-1-X) at $Q^2 = 1 \text{ GeV}^2$ with a starting optics database which was rather approximate: **db_coin_8**. At the time (1998) we worked on the y_{tg} spectrum. We calculated the predicted value of Y_{middle} = middle of the y_{tg} distribution for each choice of calset. An example is given in figure 2 for run 1531, corresponding to elastic ep kinematics with 15cm LH2 cryotarget, $\theta_{HRSE} = 15.4^\circ$ and $P_E = 3.5 \text{ GeV}/c$. It shows that "calset=0" is favoured unambiguously.

Alternatively, we could have worked on the $spec.e.reactz$ spectrum and drawn the same conclusion. This is shown in figure 3 for the same sample (run 1531).

N.B.: We were lucky that for this period of runs (ca-1-X) the difference in mispointing for the two calset choices is very large. Typically, $HPMMAG0 = 4.2 \text{ mm}$ and $HPMMAG1 = 0.5 \text{ mm}$, yielding a difference of 3.7 mm. So even with a rather bad optics the choice could be made.

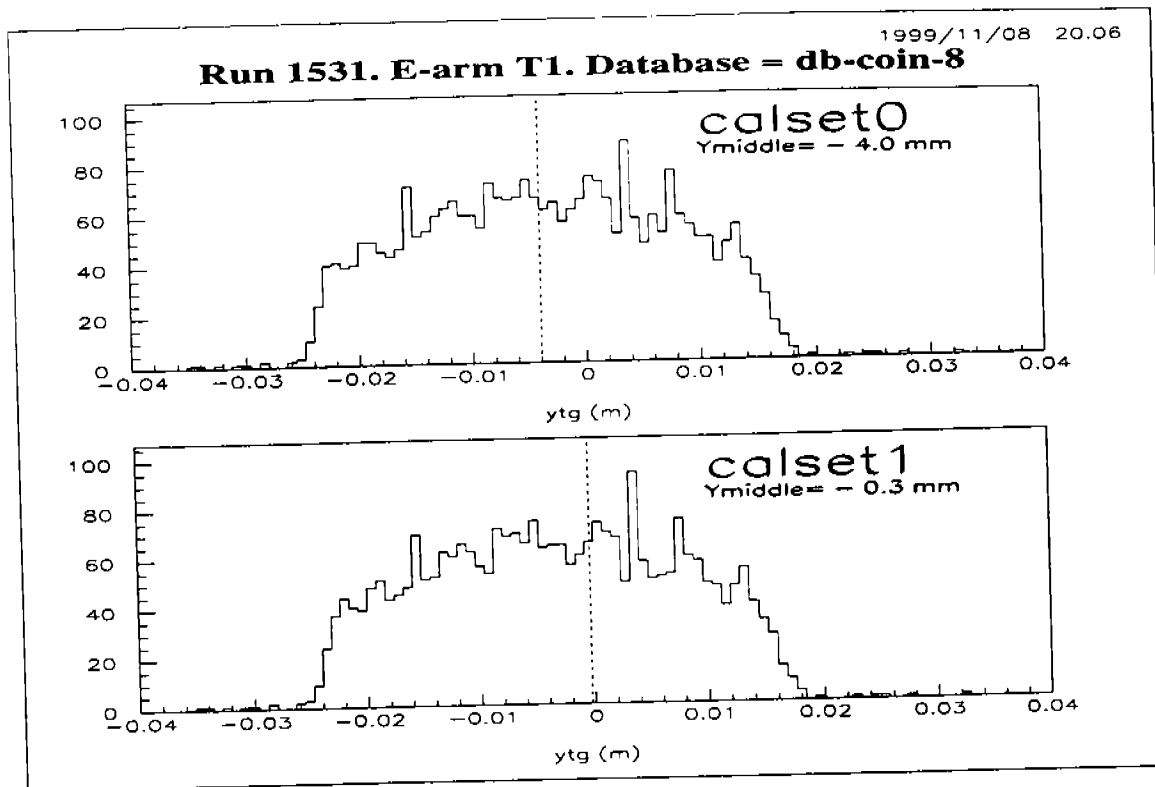


Figure 2: Example of Calset choice based on y_{tg} study for data at $Q^2 = 1 \text{ GeV}^2$. The dashed line is the predicted value of Y_{middle} using HPMMAG0 or HPMMAG1.

b). based on point a, we used HPMMAG0 to reconstruct T1 events and we did the optics optimization at $Q^2 = 1 \text{ GeV}^2$, i.e. for run numbers around 15XX. Throughout this series of runs the E-arm LVDT is very stable, so once the choice of calset has been made we can keep it. Most recent E-arm optimized optics of this kind are in **db-vcs-9m** or **-9m2**.

c). Then we moved to calibration data at $Q^2 = 2 \text{ GeV}^2$, i.e. for an Electron momentum setting $P_E = 3.0 \text{ GeV}/c$. As a starting database we used db-vcs-9m. The underlying assumption, which is legitimate, is that the E-arm optics does not change much when the momentum setting goes from 3.5 to 3.0 GeV/c .

Here, for every run used to do the optics optimization at $Q^2 = 2 \text{ GeV}^2$: empty target or sieve-slit run, we checked the choice of calset by looking at the spec.e.reactz spectrum. Results are shown in figure 4 and again they favour "calset=0" with no ambiguity.

N.B. : The difference between HPMMAG0 and HPMMAG1 is twice smaller than for runs 15XX. Typically, HPMMAG0= 5.0 mm and HPMMAG1= 3.2 mm (run 1904), yielding a difference of 1.7 mm. Then the method using spec.e.reactz becomes really more powerful than the method using y_{tg} .

d). Having made the choice "calset=0" for these calibration runs, we did the optics optimization at $Q^2 = 2 \text{ GeV}^2$. The most recent E-arm optimized optics of

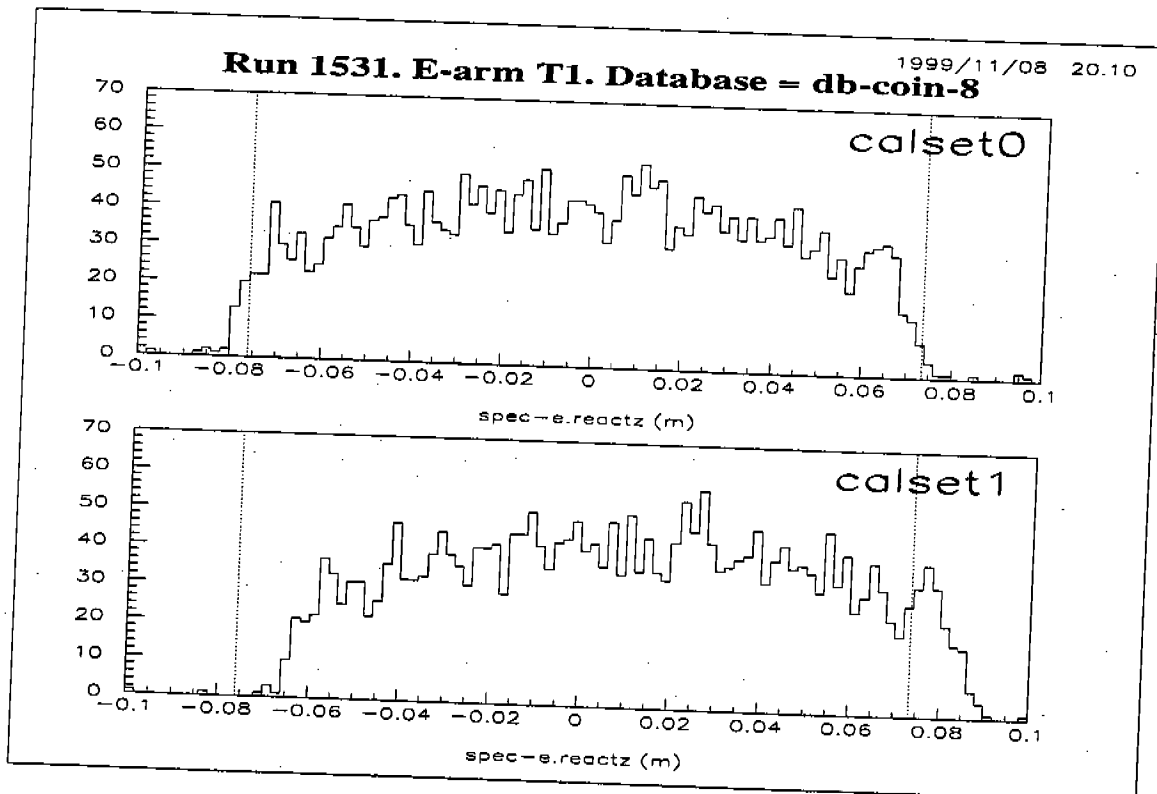


Figure 3: Example of Calset choice based on spec.e.reactz study. The dotted lines show the endcaps position as given by the 15 cm cryotarget survey: $Z_{min} = -75.9\text{mm}$, $Z_{max} = +73.6\text{ mm}$ (uncertainty is $\pm 1\text{ mm}$).

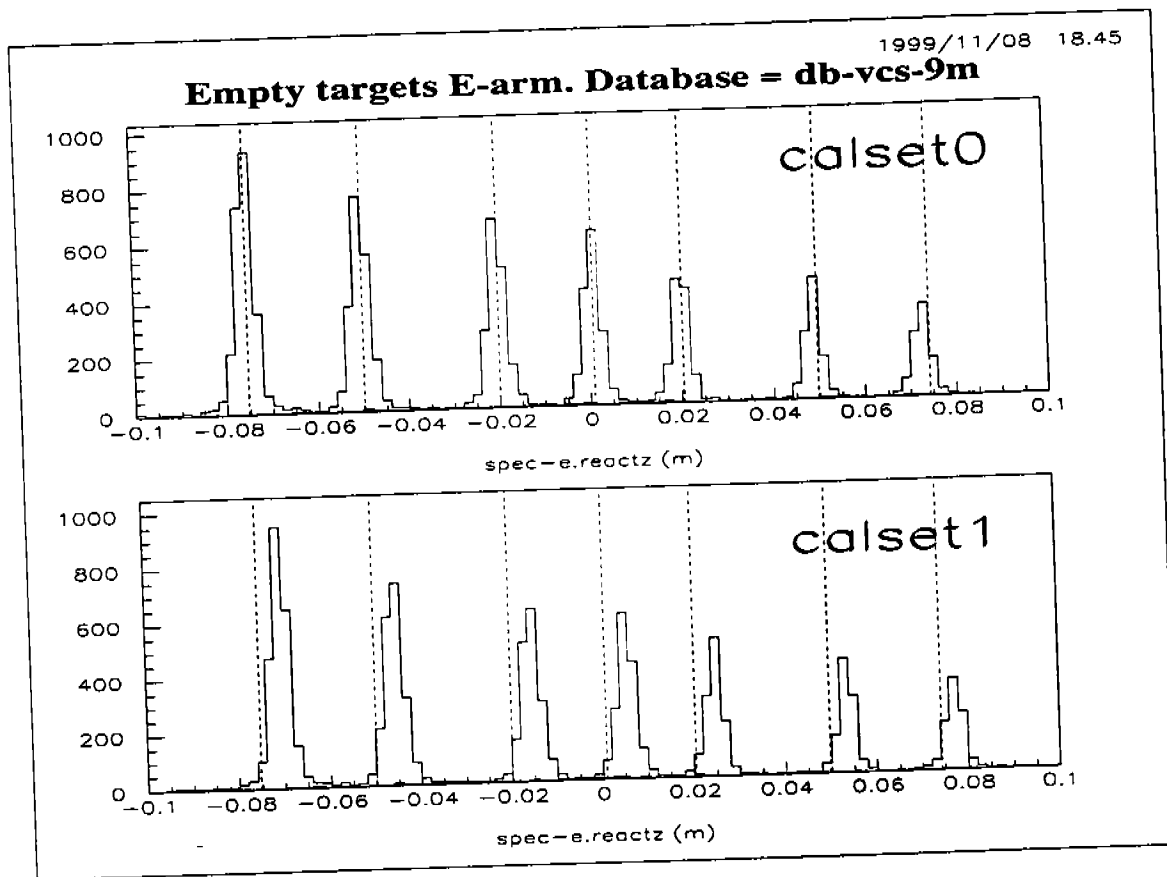


Figure 4: Example of Calset choice based on spec_e.reactz study for data at $Q^2 = 2$ GeV^2 analyzed with an optics database optimized at $Q^2 = 1$ GeV^2 . The dotted lines show the endcaps position as given by the Empty targets survey (uncertainty is $= \pm 1$ mm).

this kind is in db-vcs-10m.

Conclusion: optics database optimization in the E-arm has been a story of successive steps, each step relying on the findings of the previous one. We have shown that the whole chain is consistent.

5 Proposed Method to choose the calset for a given run

There are periods of runs in E93050 where the choice of calset is not yet clear up to now. To apply the single-arm method to such cases:

1. run Espace on a large sample of T1 events for your run number.
2. save in Espace Ntuple: beamx, and Electron Arm variables : y_{tg} , ϕ_{tg} , θ_{tg} , spec_e.dp (and possibly beamy, bpmbxraw, ..., to make cross checks if you want).
3. make standard cuts in E-arm variables other than y_{tg} (± 35 mr in ϕ_{tg} , ± 60 mr in θ_{tg} , etc).
4. compute the variable spec_e.reactz for the two choices of calset. Beware, Espace calculation is not correct because it is done before extended target corrections. Although it may not introduce a big error, it is preferable to compute the vertex variables at the correct level.
5. make the plots of spec_e.reactz for the two choices of calset.

One should be able to choose the calset just by eye, without any fitting procedure: *the correct choice is the one which gives the best centering of the experimental spectrum w.r.t. the survey of the 15cm cryotarget.*

An example is given in figure 5 where the difference in mispointing is one of the smallest ever found: $HPMMAG0 - HPMMAG1 = 1.1$ mm. Left (right) plots show the lower (upper) edges of the spec_e.reactz spectrum for the two choices of calset. The vertical lines are the endcaps position given by target survey, within their estimated error of ± 1 mm. The obvious choice is "calset=1"³.

³This confirms that indeed there has been at last one change of calibration set during E93050.

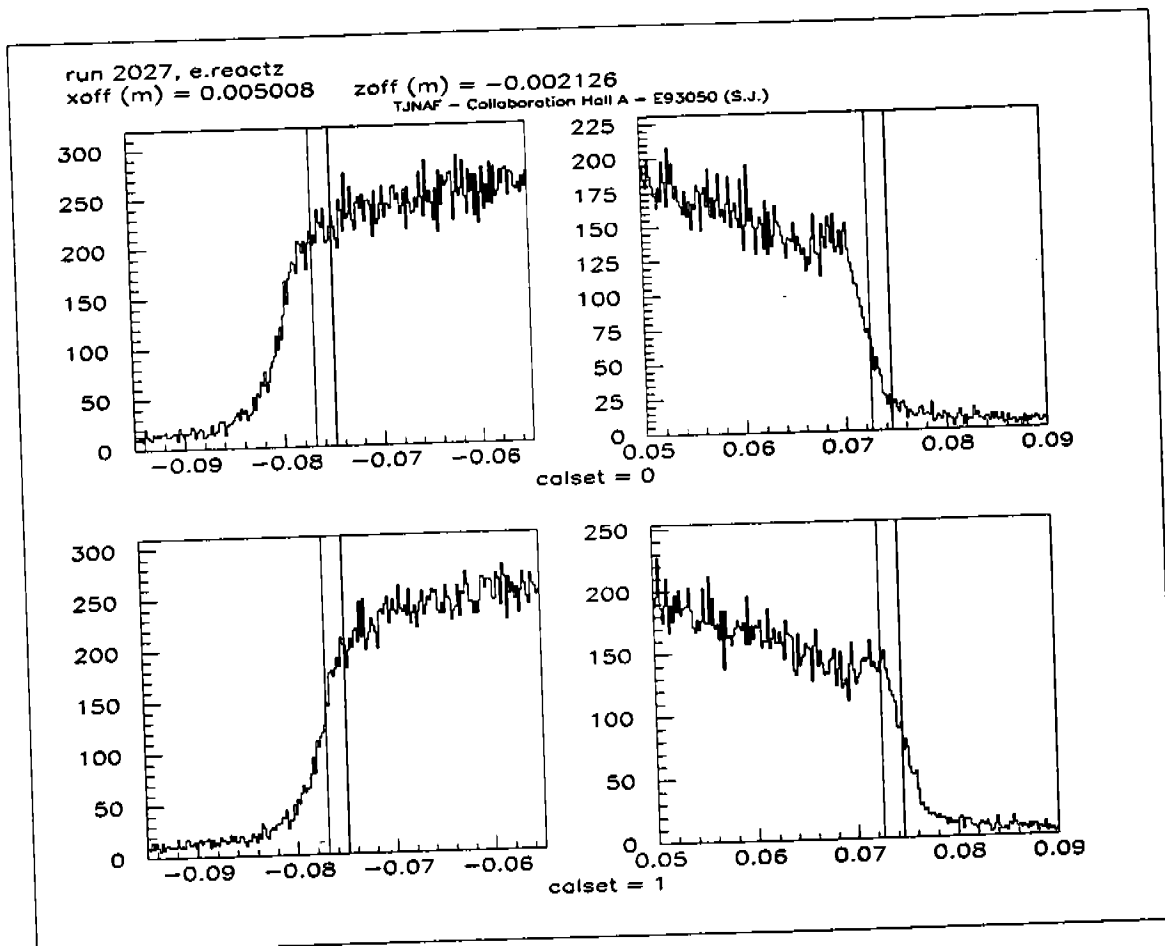


Figure 5: Example of spec.e.reactz spectrum for calset=0 (TOP) and calset=1 (BOTTOM) together with the target survey (lines). Software provided by Stephanie.

6 Usage

Stephanie has provided a software to use this single-arm method:

~/jaminion/calset/README.TXT	(notes explicatives)
/calset_choice.kumac	(le kumac)
/2027.hbook	(fichier contenant le ntuple)
/calset_2027.ps	(le postscript sortant)

7 Conclusion

The single arm method based on spec.e.reactz spectrum seems to be able to disentangle between calset=0 and calset=1 in the Electron Arm even when the difference in mispointing is as small as 1 mm (which may still be of concern for E93050 analysis). Of course, the diagnostic gets easier when the difference (HPMMAG0 - HPMMAG1) grows bigger.

There are runs where we have no confidence in either choice of calset, because they give mispointing values in the E-arm which are far from the allowed physical range (max. ~ 4 mm dicit J.Gomez. EPICS data gives 5 to 6 mm in some cases). For these runs, one should try various HPMMAG values and choose the one which corresponds to the best centering of the spec.e.reactz spectrum w.r.t. the cryotarget survey. Based on the last example presented in this memo, an accuracy of better than 1 mm seems reachable in the determination of the true HPMMAG in the Electron Arm.

E93050

HRS Optics Optimization with extended targets

Minimisation formulas for optics calibration runs :

Sieve-slit and Empty Targets runs

H. Fonvieille, LPC-Clermont

August 1999

Updated September 2000

This note summarizes the HRS optics optimization method developed at LPC-Clermont for Jlab E93050 Expt.

1 Context

A good knowledge of the optics of Hall A HRS spectrometers is crucial for good event reconstruction. This optical tensor is determined empirically using specific calibration data. The Hall A analyzer ESPACE was the first tool designed to perform this optimization. The need for a new optimization method emerged with the use of extended targets. We describe the principle of the optics optimization of tensor elements Y, T and P performed at Clermont-Fd for Experiment E93050 (15cm long hydrogen target). Unfortunately the code has not been developed in a very user-friendly way and simply cannot be distributed widely. Thanks to Nilanga Liyanage, who has developed in year 2000 at Jlab a stand-alone optimization program that runs downstream of ESPACE and does a similar job. This note was intended to provide detailed formulas and guideline for his optimization code.

2 Introduction

Notations: spectrometer frame is in Transport convention. The use of Hall A frame is necessary as soon as one wants to couple beam information with spectrometer information. cf figure 1 for frame definitions. Going from spectrometer frame to Hall A frame involves the knowledge of spectrometer angle: θ_{spec} and spectrometer mispointing.

Optical reconstruction: In each arm it gives four variables characterizing the track at the target: relative momentum dp/p , vertical angle θ_{tg} , horizontal angle ϕ_{tg} and horizontal coordinate y_{tg} in spectrometer frame.

$$\begin{aligned}
dp/p &= \sum_{jkli} D_{jkli} \times \theta_{fpr}^j y_{fpr}^k \phi_{fpr}^l x_{fpr}^i \\
\theta_{tg} &= \sum_{jkli} T_{jkli} \times \theta_{fpr}^j y_{fpr}^k \phi_{fpr}^l x_{fpr}^i \\
y_{tg} &= \sum_{jkli} Y_{jkli} \times \theta_{fpr}^j y_{fpr}^k \phi_{fpr}^l x_{fpr}^i \\
\phi_{tg} &= \sum_{jkli} P_{jkli} \times \theta_{fpr}^j y_{fpr}^k \phi_{fpr}^l x_{fpr}^i
\end{aligned} \tag{1}$$

Interaction point: using the reconstruction of one spectrometer and the beam location on target: *beamX*, *beamY* (usually expressed in Hall A frame) one can also have an experimental determination of the interaction point in 3D: (x_V, y_V, z_V) in Hall A frame. To do that: 1) in horizontal projection, cross the beam trajectory with the particle trajectory. This gives (x_V, z_V). 2) Identify y_V with *beamY*. There is no other choice, since the spectrometer does not reconstruct any vertical coordinate.

From this 3D vertex point, one can find the point W along the particle trajectory where it crosses the plane [$Z=0$] of spectrometer frame. the vertical coordinate x_W (in spectrometer frame) is called x_{tg} or *ray(1)* in Espace and is useful for calculations below.

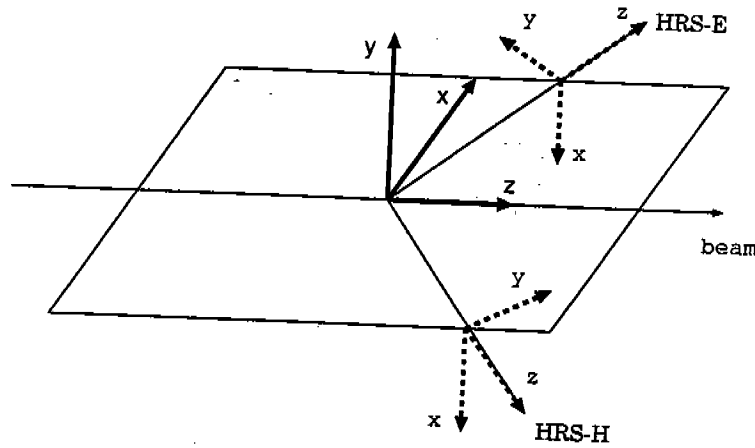


Figure 1: Orientation of Hall A frame and spectrometer Transport frame. (the three origins have been split for clarity.)

3 Sieve-Slit runs

Principle: For a point-like target, one takes data (single-arm, elastic) with a sieve slit placed just before the spectrometer entrance. The pattern in reconstructed (θ_{tg}, ϕ_{tg}) is a series of holes and one minimizes the size of holes and constrains the location of their centroid.

New method: For an extended target the pattern of reconstructed (θ_{tg}, ϕ_{tg}) in sieve-slit data is no longer a series of holes, because particles passing through a hole come from a large range of horizontal angles ϕ_{tg} . So one has to go directly to the sieve-slit plane and do the minimization on reconstructed hole profiles ¹ in 2D.

Optimization of T_{jkli} and P_{jkli} tensor elements is obtained by minimizing a chi-square between the impact coordinates of the track in the sieve-slit plane (x_S, y_S) and the theoretical position of the center of the sieve holes (x_{theo}, y_{theo}) .

Calculation of impact coordinates (x_S, y_S) :

$$\begin{aligned} x_S &= D * \theta_{tg} + x_{tg} && \text{(vertical coord., spectrometer frame)} \\ y_S &= D * \phi_{tg} + y_{tg} && \text{(horizontal coord., spectrometer frame)} \end{aligned} \quad (2)$$

D is the distance from origin of spectrometer frame to Sieve-slit plane (target side). x_{tg} involves the knowledge of beam position on target and spectrometer mispointing in 3D as contained in Espace headerfile:

```
spece_offset r 3 Xoff Yoff Zoff
```

The spectrometer angle θ_{spec} will be taken positive in both arms. *beamX* axis is positive towards E-arm. *beamY* axis is positive upwards. x_S axis is positive downwards in both arms. y_S axis is positive when going away from the beam in E-arm, and opposite convention in H-arm.

Taking into account spectrometer offsets and beam position, we get the following formulas for x_{tg} :

Electron arm:

$$x_{tg} = \left(y_{tg} + \frac{X_{off}}{\cos(\theta_{spec})} \right) \frac{\theta_{tg} \cos(\theta_{spec})}{\sin(\theta_{spec} + \phi_{tg})} - \frac{\theta_{tg} beamX}{\sin(\theta_{spec} + \phi_{tg})} - beamY + Y_{off} \quad (3)$$

Hadron arm:

$$x_{tg} = - \left(y_{tg} + \frac{X_{off}}{\cos(\theta_{spec})} \right) \frac{\theta_{tg} \cos(\theta_{spec})}{\sin(\theta_{spec} - \phi_{tg})} + \frac{\theta_{tg} beamX}{\sin(\theta_{spec} - \phi_{tg})} - beamY + Y_{off} \quad (4)$$

Formulas 2, 3 and 4 display the explicit dependence of (x_S, y_S) on the target variables given by optical reconstruction, and hence on the tensor elements T,P,Y.

¹This idea was first proposed by P.Vernin, CEA-DAPNIA, in 1998.

A chi-square is formed over N events taken from a series of sieve-slit calibration runs :

$$\chi^2 = \sum_{n=1}^N \left([x_S(n) - x_{theo}(n)]^2 + [y_S(n) - y_{theo}(n)]^2 \right) \quad (5)$$

The χ^2 minimization will be expressed as:

$$\frac{\partial \chi^2}{\partial T_{jkl i}} = 0 \quad , \quad \frac{\partial \chi^2}{\partial P_{jkl i}} = 0 \quad (6)$$

for all allowed j, k, l, i . This minimization can be *linearized* w.r.t. the T and P elements provided that, in equations 3 / 4:

- one linearizes the term $(1/\sin(\theta_{spec} \pm \phi_{tg}))$. This is perfectly justified as long as ϕ_{tg} is small compared to θ_{spec} . However it creates dot product terms, i.e. terms containing $\theta_{tg} \times \phi_{tg}$.
- One assumes that for minimization w.r.t. T, in the dot product terms ϕ_{tg} is kept fixed to its value event by event.
- One assumes that for minimization w.r.t. P, in the dot product terms θ_{tg} is kept fixed to its value event by event.

Then the χ^2 can be written as:

$$\chi^2 = \sum_{n=1}^N \left([(I) + \sum_{jkl i} (II) T_{jkl i}]^2 + [(III) + \sum_{jkl i} (IV) P_{jkl i}]^2 \right) \quad (7)$$

and the minimization leads to a system of linear equations from which one extracts the T and P tensor elements. Each parenthesis (I) to (IV) is a sum over the N events of various functions of the event variables, including: y_{tg} , $beamX$, $beamY$, D , θ_{spec} , X_{off} , x_{theo} , y_{theo} .

4 Empty target runs

Principle: one takes data (single-arm, elastic or quasielastic) for a series of thin targets spaced along the beam axis. The pattern in reconstructed z_{tg} (= vertex point coordinate along beam axis) is a series of peaks corresponding to the foils. One minimizes the peak width and constrains the location of their mean value.

New method: For a thin foil located at the center ($z = 0$), the acceptance in ϕ_{tg} is symmetric: e.g. $[-30, +30]$ mr. The foil centroid on z and y_{tg} axis are related simply by: $\bar{y} = \bar{z} * \sin \theta_{HRS}$ (up to offsets and beam position).

For a thin foil located far from the center (e.g. $z = 75$ mm) the acceptance in ϕ_{tg} is no longer symmetric: e.g. $[-10,+35]$ mr. The foil centroid on z and y_{tg} axis are related by: $\bar{y} = \bar{z} * \sin(\theta_{HRS} + \bar{\phi}_{tg})$ with $\bar{\phi}_{tg} \neq 0$. We don't know how ESPACE optimization deals with this geometrical property. In our new method, the exact relation between z_{tg} , y_{tg} and ϕ_{tg} is used event by event.

Optimization of Y_{jkli} tensor elements is obtained by minimizing a chi-square between the z_V coordinate of the interaction point and the theoretical position z_{theo} of the thin target foils along the beam axis.

Calculation of z_V coordinate event per event:

Electron Arm:

$$z_V = - \left(y_{tg} + \frac{X_{off}}{\cos(\theta_{spec})} \right) \frac{\cos(\phi_{tg})}{\sin(\theta_{spec} + \phi_{tg})} + \frac{beamX}{\tan(\theta_{spec} + \phi_{tg})} \quad (8)$$

Hadron Arm:

$$z_V = \left(y_{tg} + \frac{X_{off}}{\cos(\theta_{spec})} \right) \frac{\cos(\phi_{tg})}{\sin(\theta_{spec} - \phi_{tg})} - \frac{beamX}{\tan(\theta_{spec} - \phi_{tg})} \quad (9)$$

These formulas display the explicit dependence of (z_V) on the tensor elements Y . A chi-square is formed over N events taken from a series of empty target runs:

$$\chi^2 = \sum_{n=1}^N \left([z_V(n) - z_{theo}(n)]^2 \right) \quad (10)$$

and the χ^2 minimization is expressed as:

$$\frac{\partial \chi^2}{\partial Y_{jkli}} = 0 \quad \text{for all allowed } j, k, l, i. \quad (11)$$

As can be seen from equations 8 / 9, the minimization w.r.t. Y is linear and there is no need to make approximations like in the previous section for (T,P).

5 General remarks

Y optimization: first, it should be pointed out that the empty target runs do not allow to optimize P elements but only the Y. Although the P's are present in equation 8 via ϕ_{tg} , it turns out that z_V is not highly sensitive to ϕ_{tg} . Furthermore, z_V does not depend on vertical angle θ_{tg} .

So, Y optimization with empty target runs should be done first among all four optimizations: Y,T,P,D.

(T,P) optimization: this one needs that y_{tg} is already well reconstructed. Indeed in the expression of y_S of equation 2, the contributions of y_{tg} and of $D * \phi_{tg}$ are of the same order of magnitude.

D optimization: it needs that ϕ_{tg} is already well reconstructed. This should be done as the last of the four optics optimizations.

Convergence: in principle, the minimizations explained above are linear w.r.t. the tensor elements, so one should reach the optimized values of T,P, or Y in one single step. However, the convergence process is slowed down, mostly because of the presence of extended target corrections. One can see it in the fact that, on the right-hand side of equation 1, the focal plane variables x_{fpr} etc ... are themselves dependent on the optical tensor. Why it is so can be understood by recalling the reconstruction scheme used with an extended target:

1. get $(x, y, \theta, \phi)_{detector}$ from the VDC tracking.
2. get $(x, y, \theta, \phi)_{fpr}$ in Transport rotated frame using the p000, t000, y000 coefficients.
3. get $(dp/p, y, \theta, \phi)_{tg}$ by equation 1, first pass.
4. determine vertical extension of track at target ($ray(1) = x_{tg}$).
5. get new $(x, y, \theta, \phi)_{fpr}$ induced by this x_{tg} .
6. get new $(dp/p, y, \theta, \phi)_{tg}$ by equation 1, second pass.

In equation 1, the focal plane variables are the ones of item 5. Thus they depend on x_{tg} , which depends on 1st pass target variables, which in turn depend on the optics.

Other reasons for slow convergence: i) as tensor elements are getting optimized, events are reconstructed with different values of target variables. New events will be accepted within fixed cuts (e.g. cuts around foil peaks or around sieve holes center) and will enter the chi-square. ii) in the case of (T,P) optimization, approximations were made to linearize the system of equations.

So for all these reasons it is necessary to make several iterations in each type of chi-square minimization.

Detector offsets: the p000, t000, y000 coefficients are NOT fitted by these methods. The above minimizations assume that detector offsets are fixed and well known. We have developed a dedicated method to optimize the detector offsets. It uses the analytical formulas relating the focal plane coordinates $(x, y, \theta, \phi)_{det}$ in detector frame, to the focal plane coordinates $(x, y, \theta, \phi)_{rot}$ in Transport rotated frame. It selects events in a phase space where these formulas can be linearized w.r.t. the p000, t000, y000 coefficients. For these events, a minimization can then be written based on the known constraints on z_V , or

(x_S, y_S) like for the Y,T,P optimization. This is performed on [Sieve-slit data + empty target data] in a coupled way.

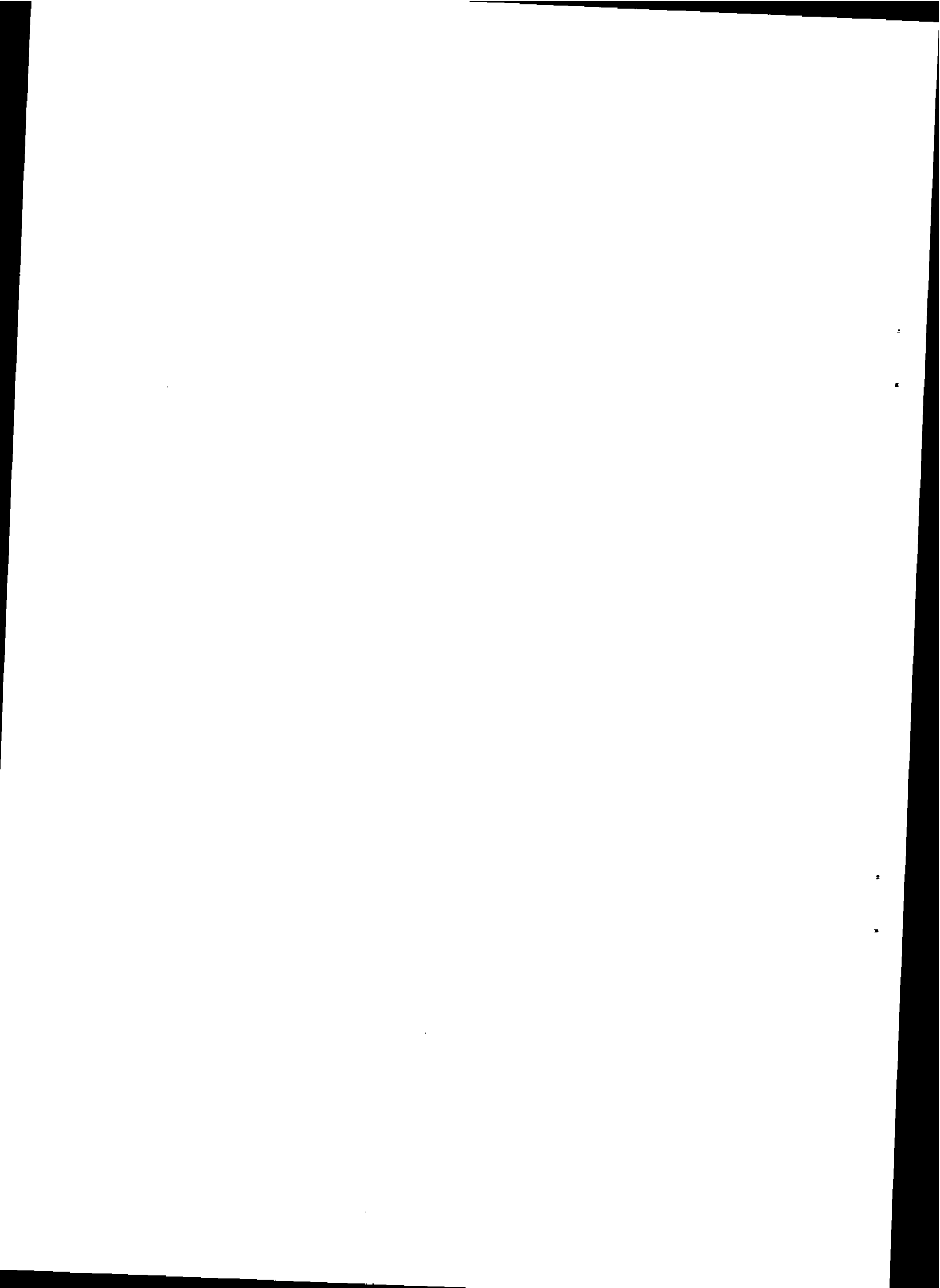
Optical tensor: maximal order and symmetry laws. Up to now (year 2000, 1st pass analysis E93050) Y,T,P elements have been optimized up to order 4. More specifically, in eq.(1) we have set $i + j + k + l \leq 4$.

The only terms allowed by spectrometer mid-plane symmetry are the following:

(k+1) *even* for D and T elements

(k+1) *odd* for Y and P elements.

The other terms are forbidden, e.g. Y000i. For the Electron Arm there has been no difficulty finding an optics that fulfills this symmetry. For the Hadron Arm it has not been the case up to now, and most "good optic databases" include terms violating mid-plane symmetry.



H.Fonvieille
LPC-Clermont-Fd
April 2000.

E93050

A Study of Optic Databases Resolution

This memo aims to give an estimate of the resolution attached to the HRS optic databases that we are using for the 1st pass analysis of Hall A experiment VCS-E93050. Results are given for y_{tg} , θ_{tg} and ϕ_{tg} resolution, based on the study of E93050 calibration runs. For final results see the last section.

1 Introduction

For first pass analysis we use two databases corresponding to the two sets of VCS-polarizability data, at $Q^2 = 1$ and 2 GeV^2 . In this memo I will call them **DB(Q2=1)** and **DB(Q2=2)**. They can be found e.g. on our computers at LPC-Clermont:

/users/divers/cebafe/vcs/softspace/db/pgq2.1/det1/db_lpc.1
/users/divers/cebafe/vcs/softspace/db/pgq2.2/det1/db_lpc.1

or on Jlab computers:

/home/helene/e93050/db/pgq2.1/det1/db_lpc.1
/home/helene/e93050/db/pgq2.2/det1/db_lpc.1

and they correspond to the following HRS angle and momentum setting:

database name	Electron Arm central mom.	Electron Arm angle	Hadron Arm central mom.	Hadron Arm angle
DB(Q2=1)	3400 MeV/c	15.4°	1100 MeV/c	54°
DB(Q2=2)	2900 MeV/c	23°	1700 MeV/c	42°

In these databases the Y/T/P ($y_{tg}/\theta_{tg}/\phi_{tg}$) optimization was done at LPC-Clermont on extended target E93050 calibration runs. D elements ($\delta p/p$) have been taken from Cebaf databases compiled by Nilanga Liyanage: db_cebaf_3.0 and db_cebaf_3.5 [4].

In this memo I have studied our E93050 calibration runs in terms of the resolution attached to the optics databases. Results will be given for y_{tg} , θ_{tg} and ϕ_{tg} . We have no E93050 data that allows to extract momentum resolution.

Calibration runs used for optics optimization : all optics optimizations are single arm work, based on single arm data. In the table below is summarized the E93050 calibration data used for Y, T and P optimization.

Type of Runs for Angle and Momentum setting of DB(Q2=1)		
Empty Targets	available in E-Arm (electrons)	available in H-Arm (protons)
Quasi-elastic on nuclei	available in E-Arm (electrons)	NOT available in H-Arm
Sieve-Slits, LH2 15 cm (ep) elastic, five $\delta p/p$	available in E-Arm (electrons)	
Type of Runs for Angle and Momentum setting of DB(Q2=2)		
Empty Targets	available in E-Arm (electrons)	available in H-Arm (protons)
Quasi-elastic on nuclei	available in E-Arm (electrons)	available in H-Arm (electrons) ($\theta_{HRS} = 32^\circ$)
Sieve-Slits, LH2 15 cm (ep) elastic, five $\delta p/p$	available in E-Arm (electrons)	

2 Resolution due to spectrometer optics

When an event is reconstructed using the VDC tracking and the optical transport to the target, we would like to know what is the resolution obtained on the spectrometer variables y_{tg} , ϕ_{tg} , θ_{tg} and $\delta p/p$. In other words, how much on average do these variables differ from their *true* value, i.e. the value at vertex point when the particle was emitted.

One can split the resolution in a simple way into two contributions:

1. one due to the passage of the particle through matter between its vertex point and the entrance of the spectrometer: mostly multiple Coulomb scattering (but also straggling) in target materials and windows, up to the kapton window at Q1 entrance.
2. all the remaining part can be attributed to "optics", or intrinsic spectrometer resolution. It includes multiple Coulomb scattering at spectrometer exit, VDC tracking resolution, etc., and is implicitly present in the database coefficients.

N.B.: this separation is somewhat arbitrary and could be made another way, e.g. [target+target walls]/[all the rest]; but it won't make much difference in the numerical results I present.

To make resolution estimates, let's define observables that are ideally delta-functions centered on a known value.

- for y_{tg} : observable = position of thin foils, or dummy target endcaps along beam axis, compared to survey.

- for ϕ_{tg} : observable = YS = horizontal impact coordinate of particle in the sieve-slit plane, compared to surveyed hole center.
- for θ_{tg} : observable = XS = vertical impact coordinate of particle in the sieve-slit plane, compared to surveyed hole center ¹.
- for $\delta p/p$: observable = $P_{measured} - P_{calculated}$ where $P_{measured}$ is the measured momentum of the particle and $P_{calculated}$ is calculated in (ep) elastic kinematics, using beam energy and scattering angle of the particle. See formula in Appendix B.

Measuring the width of the observable's distribution allows to measure the resolution due to optics ². This width is of statistical nature; one can also provide an estimate of the systematic contribution to the resolution, i.e. offsets.

3 y_{tg}

In empty target runs we build the variable *spec.e.reactz* or *spec.h.reactz* event-by-event as a function of y_{tg} , ϕ_{tg} , $beamx$, and HRS mispointing offsets. See formula in appendix B. Figures 1 and 2 show the obtained spectra for E93050 empty target runs: the endcaps of dummy targets show up as seven gaussian peaks. Their fitted RMS is shown on the figures and given in table 1 column # 2, for each spectrometer setting. The quoted value is averaged over foils, and the error bar accounts for the spread between foils.

Role of multiple Coulomb scattering in target material: it plays little role in these spectra. Indeed: *i*) multiple scattering in the foil itself plays no role, because there is no lever arm w.r.t. the vertex point. *ii*) multiple scattering in the dummy target cylindrical wall has a very small effect due to the small lever arm w.r.t. the vertex point. *iii*) I calculated multiple scattering in other materials (cf. table 11), as one single layer at distance $D_{layer} \simeq 500$ mm from target center. One gets a fluctuation on beam axis equal to: $\sigma_{ZMCS} = D_{layer} * \sigma_{\theta_{proj}} / \sin \theta_{HRS}$. See Appendix A table 13 for values of $\sigma_{\theta_{proj}}$. The obtained values of σ_{ZMCS} are small, see table 1 column # 3.

N.B.: from figures 1 and 2 it is obvious that, in most cases, the RMS of peaks is larger for upstream foils ($Z < 0$) than for downstream ones. One natural explanation would be multiple scattering in the dummy target cylindrical wall, because it affects only upstream foils. But, as mentioned above, I find it has a very small effect (assuming a wall thickness of 0.2 mm.)

Role of horizontal beam rastering: except for a constant shift, I assumed that $beamx$ was reconstructed well enough event/event (to better than ~ 0.1 mm) so that it has a negligible contribution to the foil width ³.

¹in spectrometer Transport frame: X=vertical down.

²When necessary, I will unfold target multiple scattering.

³Beam position uncertainty may have been underestimated, and so the present numbers may be revised some day!

Role of ϕ_{tg} : the observable is almost insensitive to ϕ_{tg} (see formula in Appendix B) and hence the peak width is insensitive to the resolution in ϕ_{tg} .

setting	$\sigma Z_{measured}$	σZ_{MCS}	σZ_{optics}	σy_{optics}
E-Arm DB(Q2=1)	2.37 ± 0.25 mm	0.52 mm	2.31 ± 0.25 mm	0.61 ± 0.07 mm
H-Arm DB(Q2=1)	2.30 ± 0.13 mm	0.69 mm	2.19 ± 0.13 mm	1.77 ± 0.10 mm
E-Arm DB(Q2=2)	1.69 ± 0.16 mm	0.41 mm	1.64 ± 0.16 mm	0.64 ± 0.06 mm
H-Arm DB(Q2=2)	1.96 ± 0.27 mm	0.46 mm	1.91 ± 0.27 mm	1.30 ± 0.18 mm

Table 1: Resolution study on empty target runs.

Unfolding: the resolution in Z due to the optics alone is computed from $\sigma^2 Z_{optics} = \sigma^2 Z_{measured} - \sigma^2 Z_{MCS}$. See table 1 column # 4. The resolution in y_{tg} due to optics is then deduced by: $\sigma y_{optics} = \sigma Z_{optics} * \sin \theta_{HRS}$. See table 1 column # 5.

Conclusion: one gets an optics resolution in y_{tg} of **0.61-0.64** mm RMS in Electron Arm, and of **1.3-1.8** mm RMS in Hadron Arm.

Systematic errors: the main systematic error on y_{tg} comes from the uncertainty in the global absolute positioning of the target surveys along beam axis, used in the optimization. There can be a global shift on Z as large as $\Delta Z = \pm 2$ mm [1], yielding a global offset in y_{tg} equal to $\Delta Z * \sin \theta_{HRS} = \pm 0.5$ to ± 1.6 mm depending on the spectrometer angle.

4 θ_{tg} and ϕ_{tg}

In sieve-slit runs we build XS and YS = the impact coordinates of the particle at the sieve-slit plane, in horizontal and vertical. They are function of y_{tg} , ϕ_{tg} , θ_{tg} and $beam_x$, $beam_y$ and HRS mispointing offsets. See formula in Appendix B.

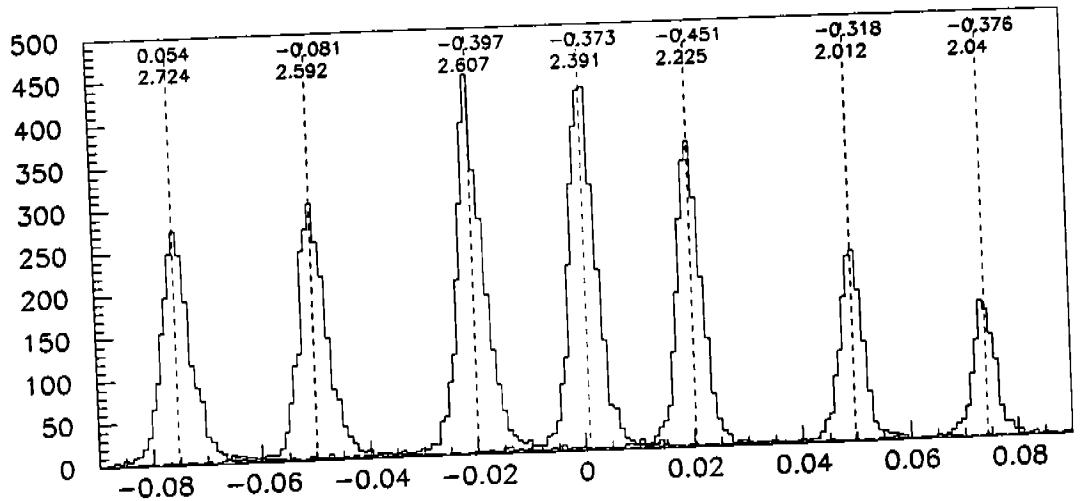
Reminder: with extended targets one cannot optimize the angles θ_{tg} and ϕ_{tg} from the distribution of these angles themselves (this is doable only for a thin target). One has to go to the sieve-slit plane and reconstruct the 2D-profiles of the holes in X and Y .

The obtained profile of the holes is gaussian in most cases. It is the convolution of a circular acceptance of diameter 4 or 2 mm, by a gaussian in X and Y due to optics resolution. This is why the observed width of the profiles changes with the hole diameter: see figures 3, 4 and 5. A simple Monte-Carlo study of this folding allows to deduce from an observed width the actual resolution in X and Y due to the optics⁴. Table 2 summarizes the obtained values. Notice the good compatibility of σ_{optics} for the different hole diameters in each case. Also very obvious from the figures is the fact that the vertical resolution is twice worse in the Hadron Arm than in the Electron Arm⁵, whereas the horizontal resolution is about the same in each arm.

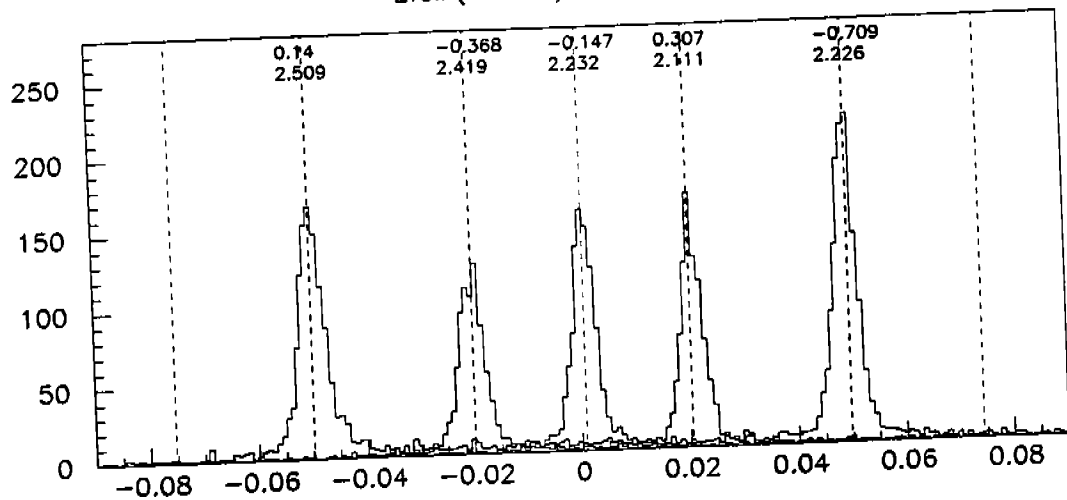
⁴like in ref. [2].

⁵(I have no explanation to this.)

E93050 Database (Q2= 1 GeV**2)



Zfoil (meters) Electron arm



Zfoil (meters) Hadron arm

Figure 1: Thin foils reconstructed on beam axis. Vertical dashed lines are the surveyed positions. First line of numbers shows the differences between fitted gaussian mean value and the survey (in mm). Second line of numbers shows the fitted gaussian RMS (in mm).

E93050 Database ($Q^2 = 2 \text{ GeV}^{*2}$)

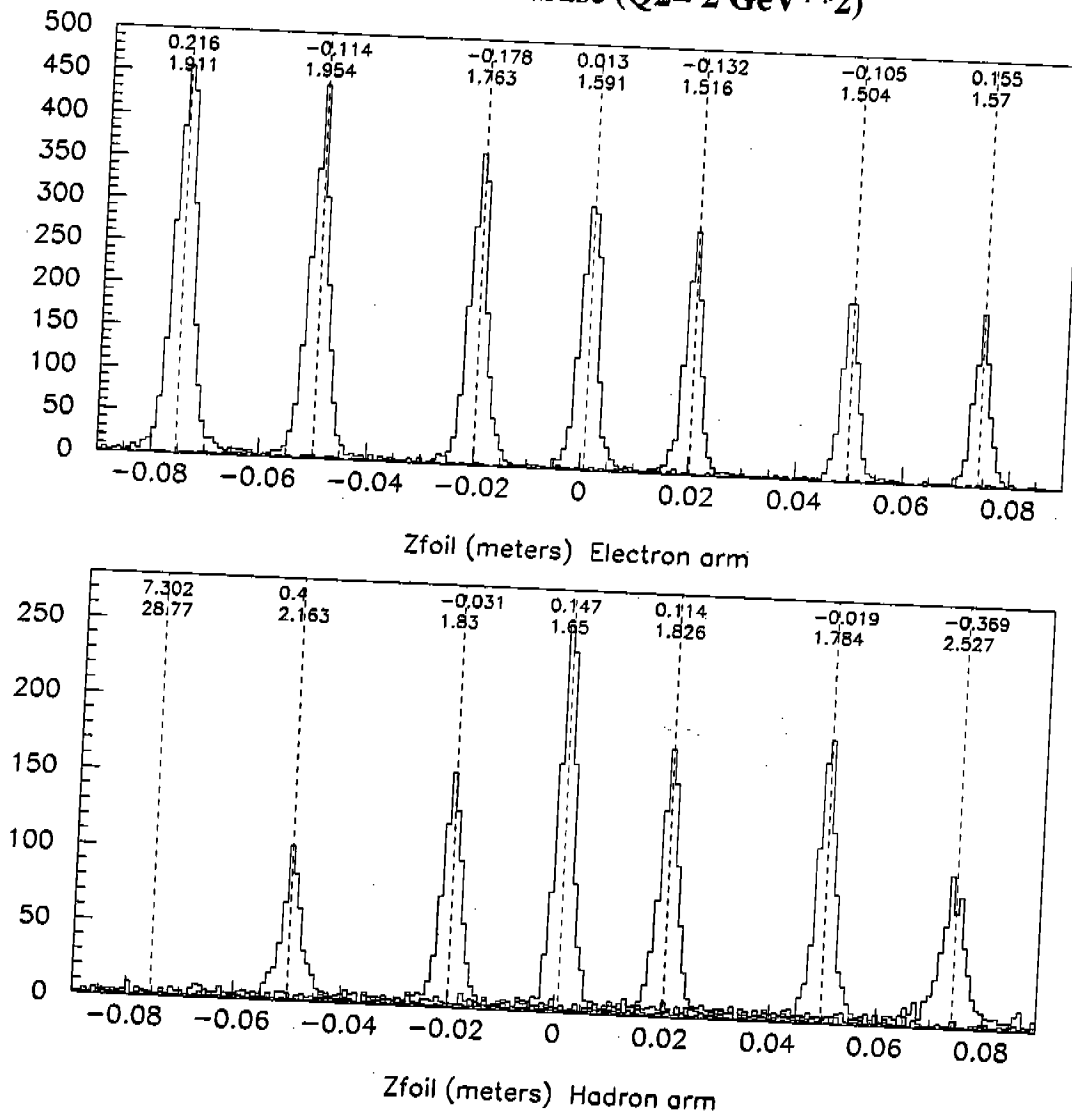


Figure 2: Same as previous figure but for $DB(Q^2=2)$.

Vertical Profile of Sieve Holes			
setting	hole diameter	$\sigma XS_{observed}$	σXS_{optics}
E-Arm DB(Q2=1)	4 mm	1.57 mm	1.20 ± 0.04 mm
	2 mm	1.29 mm	1.17 ± 0.04 mm
E-Arm DB(Q2=2)	4 mm	1.83 mm	1.53 ± 0.04 mm
	2 mm	1.56 mm	1.47 ± 0.04 mm
H-Arm DB(Q2=2)	4 mm	2.68 mm	2.51 ± 0.04 mm
	2 mm	2.68 mm	2.62 ± 0.04 mm

Horizontal Profile of Sieve Holes			
setting	hole diameter	$\sigma YS_{observed}$	σYS_{optics}
E-Arm DB(Q2=1)	4 mm	1.10 mm	0.55 ± 0.04 mm
	2 mm	0.71 mm	0.49 ± 0.04 mm
E-Arm DB(Q2=2)	4 mm	1.11 mm	0.56 ± 0.04 mm
	2 mm	0.77 mm	0.57 ± 0.04 mm
H-Arm DB(Q2=2)	4 mm	1.19 mm	0.68 ± 0.04 mm
	2 mm	0.82 mm	0.63 ± 0.04 mm

Table 2: Resolution study on Sieve Slit runs. The error bar on σ_{optics} is estimated from the Monte-Carlo.

Role of multiple Coulomb scattering in target material: it plays no role in the sieve spectra, because the observable (XS or YS) is reconstructed in a region of space that is after all target material on the particle's path. So there is no folding of target multiple scattering between the true passage in the sieve-slit plane and the reconstructed one ⁶.

A remark on the (θ, ϕ) optimization procedure: we minimize a chi-square of the type:

$$\chi^2 = \sum_{\text{events } i=1}^N [XS(i) - XS_{theo}(i)]^2 + [YS(i) - YS_{theo}(i)]^2$$

where $XS_{theo}(i)$ and $YS_{theo}(i)$ are surveyed positions of sieve hole centers. So one forces a bunch of rays filling uniformly a circular acceptance to be reconstructed as close as possible to the center of the hole. Can this bias the optics? I don't think so, as there is an averaging in each bunch of rays. Also, there would be the same kind of bias in a direct (θ, ϕ) optimization from a thin target.

Now one can extract from these results the optics resolution on the angles θ_{tg} and ϕ_{tg} .

4.1 θ_{tg}

In order to find our actual resolution in θ_{tg} , one may consider that the optimization process is formally ⁷ equivalent to determining θ_{tg} event per event by the equation:

⁶Target multiple scattering plays an indirect role, by inducing a fluctuation in x_{tg} , but it is negligible.

⁷but only formally.

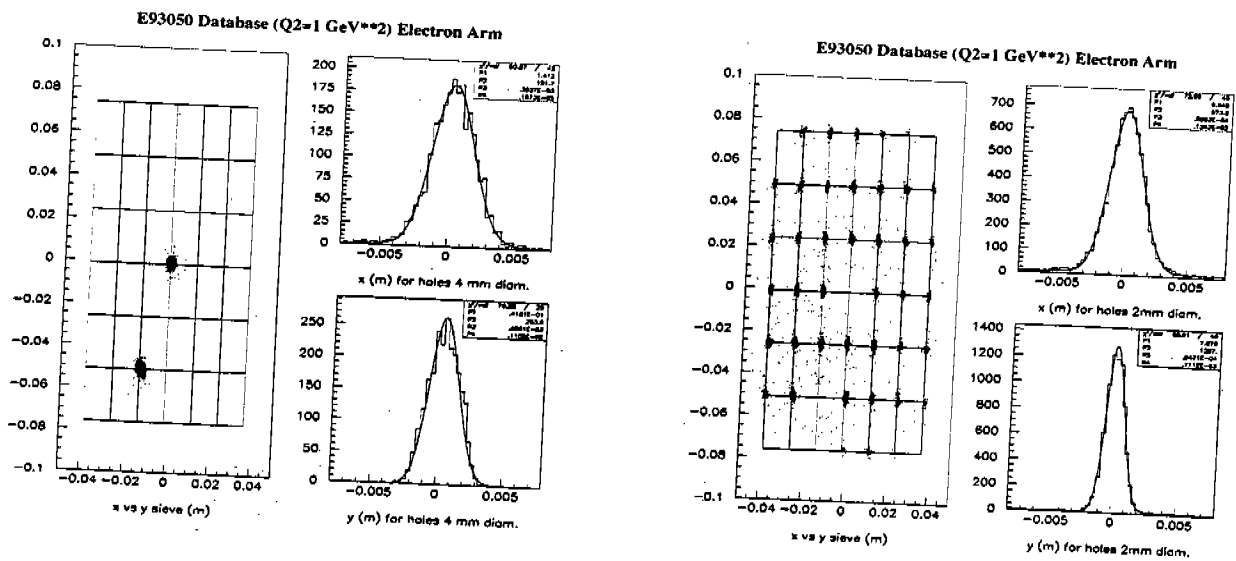


Figure 3: (X, Y) reconstruction in spectrometer Transport frame, at the sieve-slit plane for Electron Arm. Database= $DB(Q2=1)$. Left/Right = 4/2 mm diameter holes. In each case: the 2D-plot shows the survey as a grid. The 1D-plots are the vertical and horizontal profiles of the set of holes of a given diameter, w.r.t. the surveyed hole centers. The fitted function is a gaussian + flat background.

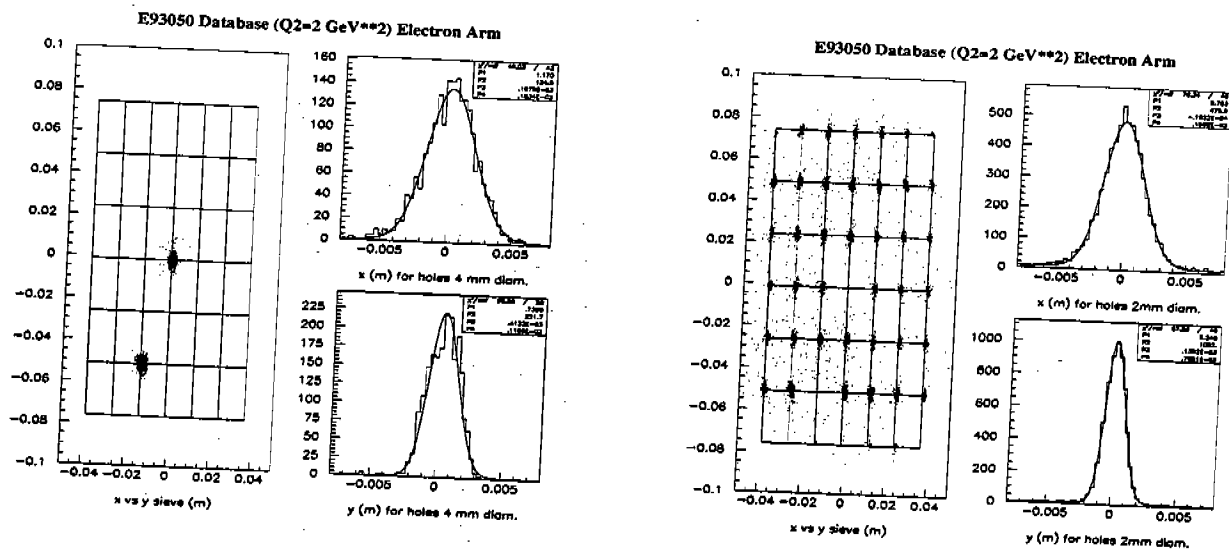


Figure 4: Same as previous figure but for Electron Arm, $DB(Q2=2)$.

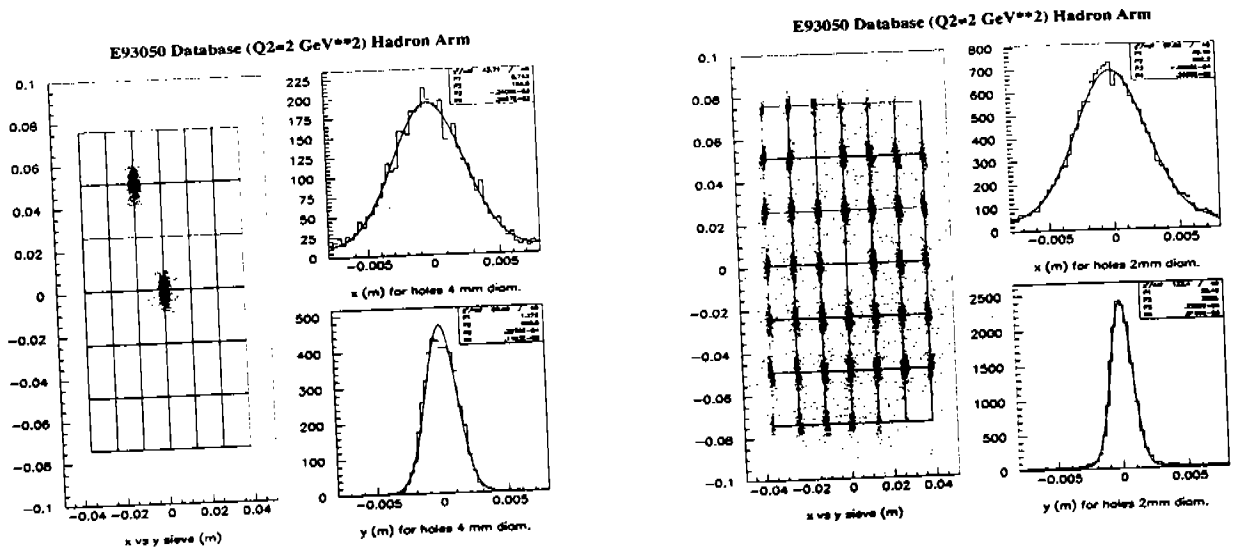


Figure 5: Same as previous figure but for Hadron Arm, $DB(Q2=2)$. N.B.: $DB(Q2=2)$ and $DB(Q2=1)$ have the same optics for Hadron Arm angles, as we had only sieve-slit data at $P=1.7$ GeV/c.

$$\theta_{tg} = (XS - x_{tg})/D_{Sieve} \quad (1)$$

where XS is as close as possible to the center of a hole in vertical. Hence the resolution in θ_{tg} is formally given by the quadratic sum:

$$\sigma^2 \theta_{tg} = \frac{1}{D_{Sieve}^2} (\sigma^2 XS + \sigma^2 x_{tg}) \quad (2)$$

Role of vertical beam rastering: except for a constant shift, I assumed that beamy was reconstructed well enough event/event (to better than ~ 0.1 mm) so that it has a negligible contribution to σx_{tg} ⁸.

Role of beam x , y_{tg} and ϕ_{tg} : they appear in x_{tg} but weighted by θ_{tg} so their role is negligible.

Actually in equation 2 the resolution in x_{tg} is always negligible so one can forget the second term. We take for σXS the value σXS_{optics} of table 2. Then we simply compute the resolution on θ_{tg} due to the optics by: $\sigma \theta_{optics} = \sigma XS_{optics}/D_{Sieve}$. See table 3 column #4.

4.2 ϕ_{tg}

We proceed exactly along the same line as for θ_{tg} . The optimization process is formally equivalent to determining ϕ_{tg} event per event by the equation:

$$\phi_{tg} = (YS - y_{tg})/D_{Sieve} \quad (3)$$

⁸same remark as in previous section on beam uncertainty.

setting	D_{Sieve}	$\sigma X S_{optics}$	$\sigma \theta_{tg} \text{ optics}$
E-Arm DB(Q2=1)	1183 mm	1.17 ± 0.04 mm	0.99 ± 0.03 mr
E-Arm DB(Q2=2)	1183 mm	1.47 ± 0.04 mm	1.24 ± 0.03 mr
H-Arm DB(Q2=2)	1174 mm	2.62 ± 0.04 mm	2.23 ± 0.03 mr

Table 3: Resolution on vertical angle at target. Reminder: H-Arm DB(Q2=1) is the same as H-Arm DB(Q2=2).

where YS is as close as possible to the center of a hole in horizontal. Hence the resolution in ϕ_{tg} is formally given by the quadratic sum:

$$\sigma^2 \phi_{tg} = \frac{1}{D_{Sieve}^2} (\sigma^2 YS + \sigma^2 y_{tg}) \quad (4)$$

Role of horizontal beam rastering: same as in section 3.

Role of vertical beam rastering: negligible effect on non-dispersive variables.

Role of y_{tg} : it is an important contribution in equation 4 and cannot be neglected.

One takes for σYS the value $\sigma Y S_{optics}$ of table 2, and for σy_{tg} the value σy_{optics} of table 1. The obtained optics resolution on ϕ_{tg} is given in table 4 column #3.

setting	$\sigma Y S_{optics}$	$\sigma \phi_{tg} \text{ optics}$
E-Arm DB(Q2=1)	0.49 ± 0.04 mm	0.65 ± 0.06 mr
E-Arm DB(Q2=2)	0.57 ± 0.04 mm	0.72 ± 0.06 mr
H-Arm DB(Q2=2)	0.63 ± 0.04 mm	1.23 ± 0.06 mr

Table 4: Resolution on horizontal angle at target. Reminder: H-Arm DB(Q2=1) is the same as H-Arm DB(Q2=2).

Conclusion: one gets an optics resolution in θ_{tg} of about 1 mr RMS in Electron Arm and 2 mr RMS in Hadron Arm. For ϕ_{tg} , we find an optics resolution of about 0.7 mr RMS in Electron Arm and 1.2 mr RMS in Hadron Arm.

Systematic errors: The systematic error on θ_{tg} and ϕ_{tg} are dominated by the uncertainty in the survey of the sieve-slit, used in the optimization. Survey measurements done in 1997 and 1999 disagree by 3 mm in vertical (E-arm). So one may have an offset in θ_{tg} of a few mr in any database. For the same reason, an offset in ϕ_{tg} of about 1 mr is not excluded.

4.3 Resolution in particle transverse coordinates along $Z_{spectro}$

We may now ask the question: suppose we need to calculate the transverse coordinates (X,Y) of the particle along its trajectory at a given depth Z_1 , e.g. +1.1 m (= 6 msr collimator plane), or -1 m (upstream of target), or elsewhere ..., where Z is measured along the spectrometer optical axis. What do we get as (optics) resolution on these coordinates? In other words, what is the shape of the resolution curve $\sigma X(Z)$ (resp. $\sigma Y(Z)$) versus Z ?

First, it is clear that these coordinates at depth Z_1 are calculated by (cf. Appendix B):

$$\begin{aligned} X_1 &= x_{tg} + Z_1 * \theta_{tg} \\ Y_1 &= y_{tg} + Z_1 * \phi_{tg} \end{aligned}$$

Horizontal coordinate Y: the way the optics optimization was made, we have actually minimized the Y resolution in two regions:

the region near $Z_{spectro} = 0$	by	y_{tg} optimization on empty target runs
the plane at $Z_{spectro} = D_{sieve}$	by	θ_{tg}, ϕ_{tg} optimization on sieve-slit runs.

so it is likely that the resolution curve $\sigma Y(Z)$ displays two minima, around $Z=0$ and at $Z=D_{sieve}$. As $D_{collimator}$ is close to D_{sieve} , one expects to have a Y resolution in the collimator plane that is about the same as $\sigma Y S_{optics}$ determined in the previous sections. This can be checked more or less by looking at reconstructed edge of 6 msr collimator⁹. Figure 6 shows a quick test done on the left edge of E-arm collimator reconstructed in an E93050 (*ep*) elastic run with DB(Q2=2)¹⁰. We find a horizontal resolution of about 0.85 mm RMS, not too far from $\sigma Y S_{optics}$.

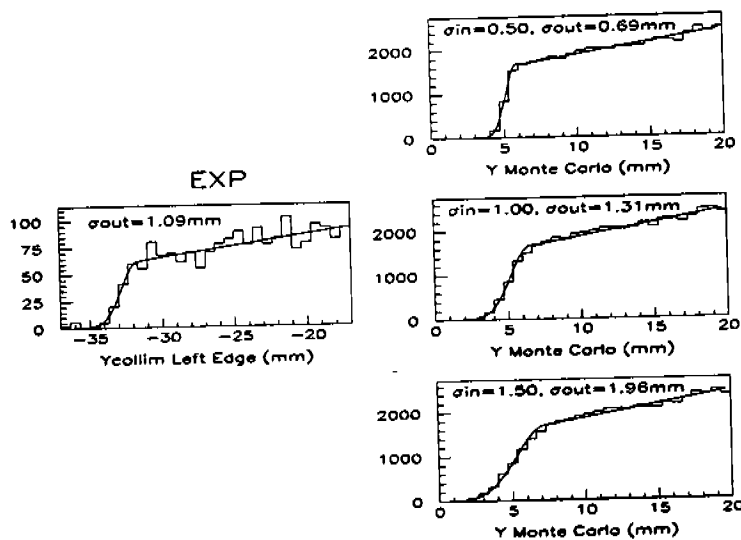


Figure 6: horizontal profile of collimator edge in Electron arm. Left = experiment. Right = Monte-Carlo folding of a step function (+slope) by a gaussian of RMS σ_{in} . σ_{out} is given by a fit. From the plotted numbers one deduces that $\sigma_{in} \simeq 0.85$ mm in experimental data.

⁹for electrons only !. The collimator cut is less sharp for protons.
¹⁰quick test means: no refined event cleaning, etc.

Vertical coordinate X : the way the optics optimization was made, we have minimized the X resolution in one fixed plane at $Z_{\text{spectro}} = D_{\text{sieve}}$. But there is also a natural minimum at $Z = 0$ where the error propagation due to the term $Z * \theta_{tg}$ is minimal. So the resolution curve $\sigma X(Z)$ probably also displays two minima. The same quick test as above, looking at the E-arm vertical collimator edge, yields a resolution of 1.7 mm RMS, not far from $\sigma X S_{\text{optics}}$.

Remark: I would say that if the (θ, ϕ) optimization is done directly on the angles, using point-like target data, the resolution in transverse coordinates at $Z=1$ meter has no reason to go through a minimum, and so the resolution in $(X, Y)_{\text{collimator}}$ should not be as good as in the databases we use.

5 $\delta p/p$

Particle momentum optimization is best performed on thin targets (to reduce multiple scattering) and of high atomic mass (because of reduced dependence of P upon scattering angle). We have no such data in E93050, all our "acceptance" runs are taken with a 15cm LH2 target. So in this section we just verify that for our acceptance runs the two effects: target multiple scattering and optics resolution on scattering angle, do indeed mask the intrinsic momentum resolution.

The observable $\Delta P = P_{\text{measured}} - P_{\text{calculated}}$ is built from (ep) elastic events, using beam energy at vertex and scattering angle of the particle. See formula in Appendix B. The measured width (RMS) of the gaussian part of the ΔP distribution ¹¹ is given in table 5 column # 2.

Role of beam energy spread: negligible.

Role of beam position $beam_x, beam_y$: negligible.

Role of multiple Coulomb scattering in target material: it is important because there is a complete folding of multiple scattering between the true momentum at the vertex point and the momentum $P_{\text{calculated}}$, via the reconstructed scattering angle. I have estimated the width of ΔP due to target multiple scattering based on materials listed in Appendix A ¹². See table 5 column #3.

Role of optics resolution on target angles: the resolution on ϕ_{tg} plays a role because it affects the particle scattering angle. The resolution on θ_{tg} has almost no effect. I have estimated the width of ΔP due to $\sigma \phi_{tg \text{ optics}}$: see table 5 column #4.

Folding: the total expected RMS width of ΔP is calculated as the quadratic sum of columns #3 and #4. See column #5.

conclusion: one can say that the above calculation roughly reproduces the observed width (to ± 0.7 MeV/c), and so optics resolution on momentum cannot be extracted from this data (as is well-known).

Systematic errors: they can be summarized by the uncertainty on the Gamma factors in the

¹¹ there is also a radiative tail in this distribution.

¹² not a very refined calculation, just for a vertex point at $Z=0$.

setting	$\sigma\Delta P_{measured}$ MeV/c	$\sigma\Delta P_{MCS}$ MeV/c	$\sigma\Delta P_{\phi optics}$ MeV/c	$\sigma\Delta P_{calc}$ MeV/c
E-Arm DB(Q2=1)	2.5 MeV/c (e) [2.2 (*)]	2.6	1.6	3.1
H-Arm DB(Q2=1)	5.8 MeV/c (p) [6.2 (*)]	3.2	4.2	5.2
E-Arm DB(Q2=2)	2.9 MeV/c (e) [2.6 (*)]	3.1	2.1	3.7
H-Arm DB(Q2=2)	4.9 MeV/c (p) [4.9 (*)]	4.4	3.4	5.5

Table 5: Momentum resolution study. The target is the LH2 15 cm cryotarget. Column #2: (e)=electron, (p)=proton. number in [(*)] is the one from reference [6].

database ($\Gamma \sim 270$ MeV/kGauss). Cf ref. [3]: $\Delta\Gamma/\Gamma \geq 3.7e-4$ in E-Arm, $5.5e-4$ in H-Arm. See also tables 7, 9.

6 Conclusions

Tables 6 to 9 summarize the present study on optics resolution and data from other studies. The results in ref. [6] are based on E93050 (*ep*) elastic data (acceptance runs). The results in ref. [5] are based on a simulation of E93050 experiment ¹³.

- The present results may serve as a comparison for future measurements of optics resolution of the HRS. We hope that this comparison will trigger some more thinking and discussions, namely the comparison between data and simulation.
- For σ_{syst} the present values are globally much larger than those of ref. [4] and [2], due to the large uncertainty I have assigned to surveys (of targets and sieve).
- Consequence: for some reconstructed variables, the width of the observed distribution may be sensitive to the systematic part of the resolution, as much as the statistical part. This is the case for e.g. the missing mass squared in E93050 (= missing mass to the detected system electron + proton) whose width is enlarged by offsets in angles, etc.

I thank Luc Van Hoorebeke, Stephanie Jaminion and Geraud Laveissiere for stimulating discussions when elaborating this memo. I thank Luminita Todor for having triggered the writing of this memo.

¹³For ref. [5] I have unfolded the "total spectrometer resolution" (section 4) from the effect of air and windows before the spectrometer (section 2).

ELECTRON ARM					σ_{stat}
momentum setting	$\sigma_{y_{tg}}$	$\sigma_{\phi_{tg}}$	$\sigma_{\theta_{tg}}$	$\sigma_{\delta p/p}$	reference
3500 MeV	0.61 mm	0.65 mr	0.99 mr		this work
3000 MeV	0.64 mm	0.72 mr	1.24 mr		this work
3500 & 3000 MeV	0.68 mm			1.28e-4	Nilanga Liyanage 1999 [4]
850 MeV	1.58 mm	0.85 mr	2.77 mr	1.71e-4	Nilanga Liyanage 1999 [4]
3500 MeV	0.75 mm	0.64 mr	1.92 mr	2.00e-4	Frederic Renard 1999 [6]
3000 MeV	0.60 mm	0.68 mr	1.74 mr	2.80e-4	Frederic Renard 1999 [6]
3500 MeV	0.21 mm	0.20 mr	0.64 mr	0.13e-4	Luc Van Hoorebeke 2000 [5]
3000 MeV	0.19 mm	0.25 mr	0.69 mr	0.11e-4	Luc Van Hoorebeke 2000 [5]

Table 6: Optics resolution (RMS) Electron Arm. Statistical part.

ELECTRON ARM					σ_{syst}
momentum setting	$\sigma_{y_{tg}}$	$\sigma_{\phi_{tg}}$	$\sigma_{\theta_{tg}}$	$\sigma_{\delta p/p}$	reference
3500 MeV	± 0.5 mm	± 1 mr	± 3 mr		this work (maximized values)
3000 MeV	± 0.8 mm	± 1 mr	± 3 mr		this work (maximized values)
3500 & 3000 MeV	± 0.3 mm	± 0.3 mr	± 0.6 mr	8.e-4	Nilanga Liyanage [3] & [2]
850 MeV	± 0.5 mm	± 0.3 mr	± 0.8 mr	4.e-4	Nilanga Liyanage [3] & [2]

Table 7: Optics resolution (RMS) Electron Arm. Systematic part.

HADRON ARM					σ_{stat}	reference
momentum setting	$\sigma_{y_{tg}}$	$\sigma_{\phi_{tg}}$	$\sigma_{\theta_{tg}}$	$\sigma_{\delta p/p}$		
1100 MeV	1.77 mm	1.23 mr	2.23 mr			this work
1700 MeV	1.30 mm	1.23 mr	2.23 mr			this work
850 MeV	1.70 mm	0.64 mr	2.90 mr	1.92e-4		Nilanga Liyanage 1999 [2]
1100 MeV	0.81 mm	0.80 mr	2.60 mr	0.43e-4		Luc Van Hoorebeke 2000 [5]
1700 MeV	0.40 mm	0.36 mr	1.18 mr	0.22e-4		Luc Van Hoorebeke 2000 [5]

Table 8: *Optics resolution (RMS) Hadron Arm. Statistical part.*

HADRON ARM					σ_{syst}	reference
momentum setting	$\sigma_{y_{tg}}$	$\sigma_{\phi_{tg}}$	$\sigma_{\theta_{tg}}$	$\sigma_{\delta p/p}$		
1100 MeV	± 1.6 mm	± 1 mr	± 3 mr			this work (maximized values)
1700 MeV	± 1.3 mm	± 1 mr	± 3 mr			this work (maximized values)
850 MeV	± 0.5 mm	± 0.15 mr	± 0.5 mr	$> 7.e-4$		Nilanga Liyanage [3] & [2]

Table 9: *Optics resolution (RMS) Hadron Arm. Systematic part.*

References

- [1] J.P.Chen, private communication, and Internal report PCCF-RI-9810 (1998).
- [2] N.Liyanage et al., *Optics Commissioning of the Hall A High Resolution Spectrometers*, MIT-LNS IR # 04/98 (1998).
- [3] N.Liyanage, *Spectrometer constant determination*, Jlab Note, october 1999.
- [4] N.Liyanage, *Optics Commissioning of the Hall A High Resolution Spectrometers*, Jlab Note, june 1999.
- [5] Luc Van Hoorebeke, *Resolution effects due to spectrometers in VCSSIM*, E93050 note, march 2000, Univ. of Gent, sous presse.
- [6] Frederic Renard and Sophie Kerhoas-Cavata, *Calibration des spectromètres pour l'expérience E93050 à Jlab: caractérisation des databases à l'aide des cinématiques élastiques*, september 1999, note CEA-SPhN, sous presse.

Appendix A

Materials before spectrometer entrance

For multiple Coulomb scattering we consider the following materials, tables 10, 11:

Target Cells or Target Foils		
material	thickness	radiation length L_0
liquid hydrogen	15 cm along beam	8720 mm
Al cylinder wall of LH2 cell	0.2 mm (=7+1 mil)	89 mm
Al downstr.endcap of LH2 cell	0.1 mm	89 mm
Al cylinder wall of Dummy Targets (4,10,15 cm long)	0.2 mm (=7+1 mil) (I assume)	89 mm
Al endcaps of Dummy Targets (4,10,15 cm long)	0.31, 0.93, 0.98 mm (upstr. or downstream)	89 mm
^{12}C Solid Target	0.96 mm along beam	188 mm

Table 10:

Other Materials		
material	thickness	radiation length L_0
Al scatt.chamber window	0.4 mm	89 mm
Air gap	500 mm	3.e+5 mm
Kapton window (Q1 entrance)	0.18 mm	300 mm

Table 11:

Approximate formula for projected RMS angle of multiple Coulomb scattering in a material of thickness L and radiation length L_0 :

$$\sigma_{\theta_{proj}} = \frac{14}{p\beta} \sqrt{\frac{L}{L_0}} (1 + 0.038 \ln \frac{L}{L_0})$$

Once for all we compute $\sigma_{\theta_{projected}}$ for electrons and protons, database momentum settings and materials of tables 1 and 2, using the above formula. See tables 12, 13.

Appendix B

Formulas for some reconstructed variables

for Empty Target Data:

15 cm LH2 Target Cell + Target Walls				
setting	momentum	HRS angle	cumulated L/L_0	σ_{proj}
E-Arm DB9	3400 MeV/c	15°	(78/8720)+(0.10/89)	0.34 mr
H-Arm DB9	1100 MeV/c	54°	(39/8720)+(0.25/89)	1.16 mr
E-Arm DB10	2900 MeV/c	23°	(81/8720)+(0.11/89)	0.41 mr
H-Arm DB10	1700 MeV/c	43°	(46/8720)+(0.30/89)	0.73 mr

Table 12: Lengths L are calculated for a vertex point at $Z=0$.

Other Materials (Al.Scatt.chamb.+Air+Kapton)				
setting	central momentum	HRS angle	cumulated L/L_0	σ_{proj}
E-Arm DB9	3400 MeV/c	15°	6.76e-3 (7.08e-3)	0.27 mr (0.26)
H-Arm DB9	1100 MeV/c (1000)	54°	6.76e-3 (7.08e-3)	1.11 mr (1.28)
E-Arm DB10	2900 MeV/c	23°	6.76e-3 (7.08e-3)	0.32 mr (0.30)
H-Arm DB10	1700 MeV/c	43°	6.76e-3 (7.08e-3)	0.63 mr (0.60)

Table 13: columns 2,4 and 5: in parenthesis are Luc Van Hoorebeke's equivalent numbers in his study of resolution [5].

$$Z = \text{spece.reactz} = \frac{\text{beamx} - X_{offE} - y_{tgE} \cos \theta_{HRSE}}{\tan(|\theta_{HRSE}| + \phi_{tgE})} - y_{tgE} \sin |\theta_{HRSE}| + Z_{offE}$$

$$Z = \text{spech.reactz} = \frac{\text{beamx} - X_{offH} - y_{tgH} \cos \theta_{HRSH}}{-\tan(|\theta_{HRSH}| - \phi_{tgH})} + y_{tgH} \sin |\theta_{HRSH}| + Z_{offH}$$

First order approximation

$$\begin{aligned} (\text{beam}=0, \text{offsets}=0, \phi_{tg}=0): \quad & \text{spece.reactz} = -y_{tgE} / \sin |\theta_{HRSE}| \\ & \text{spech.reactz} = y_{tgH} / \sin |\theta_{HRSH}| \end{aligned}$$

beamx = horizontal beam position in Hall A frame

X_{off}, Z_{off} = spectrometer mispointing as expressed in Espace headerfiles, i.e. projected on X and Z axis of Hall A frame.

y_{tg}, ϕ_{tg} = spectrometer variables, in spectrometer (Transport) frame.

θ_{HRS} = nominal spectrometer angle.

for Sieve Slit Data:

$$\begin{aligned} x_{Sieve} &= x_{tg} + D_{Sieve} * \theta_{tg} && \text{(vertical)} \\ y_{Sieve} &= y_{tg} + D_{Sieve} * \phi_{tg} && \text{(horizontal)} \end{aligned}$$

$$x_{tgE} = \frac{\theta_{tgE} * (y_{tgE} \cos \theta_{HRSE} + X_{offE} - beamx)}{\sin(|\theta_{HRSE}| + \phi_{tgE})} - beamy + Y_{offE}$$

$$x_{tgH} = \frac{\theta_{tgH} * (-y_{tgH} \cos \theta_{HRSH} - X_{offH} + beamx)}{\sin(|\theta_{HRSH}| - \phi_{tgH})} - beamy + Y_{offH}$$

First order approximation

(beam=0, offsets=0, $\phi_{tg}=0$):

$$x_{tgE} = \theta_{tgE} * y_{tgE} / \tan(|\theta_{HRSE}|)$$

$$x_{tgH} = -\theta_{tgH} * y_{tgH} / \tan(|\theta_{HRSH}|)$$

$beamy$ = vertical beam position in Hall A frame

Y_{off} = spectrometer vertical mispointing as expressed in Espace headerfile.

θ_{tg} = spectrometer variable, in spectrometer (Transport) frame.

D_{Sieve} = nominal distance from Hall A center to entrance Sieve plane.

for Acceptance Data:

Measured momentum of the outgoing particle:

$$P_e \text{ measured} = P_e \text{ central} * (1. + (\frac{\delta p}{p})_e)$$

+ corrections for ionization energy loss in target
→ momentum at vertex point

$$P_h \text{ measured} = P_h \text{ central} * (1. + (\frac{\delta p}{p})_h)$$

+ corrections for ionization energy loss in target
→ momentum at vertex point

Calculated momentum of the outgoing particle in (ep) elastic kinematics:

E-Arm: $P_e \text{ calculated} = \frac{E_{beam} M_p}{M_p + E_{beam}(1 - \cos \theta_{e.scatt})}$

H-Arm: $P_h \text{ calculated} = \frac{2. E_{beam} M_p \cos \theta_{h.scatt} (E_{beam} + M_p)}{(E_{beam} + M_p)^2 - (E_{beam} \cos \theta_{h.scatt})^2}$

E_{beam} = beam energy at vertex point.

M_p = proton mass.

θ_{scatt} = scattering angle of the particle, i.e. polar angle of particle momentum \vec{P} with the beam.